| | | | | | |
|---|---|---|---|---|---|
| Nakashima K, Takeuchi K, Chihara K, Horiguchi T, Sun X, Deng L, Shoji I, Hotta H, Sada K. | HCV NS5A protein containing potential ligands for both Src homology 2 and 3 domains enhances autophosphorylation of Src family kinase Fyn in B cells. | PLoS ONE | 7(10) | e46634. | 2012 |
| Yano Y, Seo Y, Miki A, Saito M, Kato H, Hamano K, Oya M, Ouchi S, Fujisawa T, Yamada H, Yamashita Y, Tani S, Hirohata S, Yoon S, Kitajima N, Kitagaki K, Kawara A, Nakashima T, Yu H, Maeda T, Azuma T, El-Shamy A, Hotta H, Hayashi Y. | Mutations in non-structural 5A and rapid viral response to pegylated interferon-α-2b plus ribavirin therapy are associated with therapeutic efficacy in patients with genotype 1b chronic hepatitis C. | Int J Mol Med | 30(5) | 1048-52. | 2012 |
| Kim SR, El-Shamy A, Imoto S, Kim KI, Ide YH, Deng L, Shoji I, Tanaka Y, Hasegawa Y, Ota M, Hotta H. | Prediction of response to pegylated interferon/ribavirin combination therapy for chronic hepatitis C genotype 1b and high viral load. | J Gastroenterol | 47(10) | 1143-51. | 2012 |
| Shoji I, Deng L, Hotta H | Molecular mechanism of hepatitis C virus-induced glucose metabolic disorders. | Front Microbiol | 2: A278 | 1-5. | 2012 |
| El-Shamy A, Shoji I, Kim SR, Ide Y, Imoto S, Deng L, Yoon S, Fujisawa T, Tani S, Yano Y, Seo Y, Azuma T, Hotta H. | Sequence heterogeneity in NS5A of hepatitis C virus genotypes 2a and 2b and clinical outcome of pegylated –interferon /ribavirin therapy. | PLoS ONE | 7(2) | e30513. | 2012 |
| Sasayama M, Shoji I, Adianti M, Jiang D-P, Deng L, Saito T, Watanabe H, Kawata S, Aoki C, Hotta H. | A point mutation at ASN-534 that disrupts a conserved *N*-glycosylation motif of the E2 glycoprotein of hepatitis c virus markedly enhances the sensitivity to antibody neutralization. | J Med Virol | 84(2) | 229-34. | 2012 |
| Nawa T, Ishida H, Tatsumi T, Li W, Shimizu S, Kodama T, Hikita H, Hosui A, Miyagi T, Kanto T, Hiramatsu N, Hayashi N, Takehara T. | Interferon-α suppresses hepatitis B virus enhancer II activity via the protein kinase C pathway. | Virology | 432(2) | 452-9 | 2012 |

| | | | | | |
|---|---|---|---|---|---|
| Sakamoto T, Tanaka Y, Kani S, Sugiyama M, Watanabe T, **Iijima S**, Murakami S, Matsuura K, Kusakabe A, Shinkai N, Sugauchi F, Mizokami M. | Mechanism of the Dependence of Hepatitis B Virus Genotype G on Co-infection with Other Genotypes for Viral Replication. | J Viral. Hepat. | | | in press. |
| Watanabe T, Sugauchi F, Tanaka Y, Matsuura K, Yatsuhashi H, Murakami S, **Iijima S**, Iio E, Sugiyama M, Shimada T, Kakuni M, Kohara M, Mizokami M. | Hepatitis C virus kinetics by administration of pegylated interferon-l in human and chimeric mice carrying human hepatocytes with variants of the IL28B gene. | Gut | | | 2012 Nov 7. [Epub ahead of print] |
| Liu HM, Aizaki H, Machida K, Ou JH, Lai MM. | Hepatitis C virus translation preferentially depends on active RNA replication. | PLoS One | 7 | e43600 | 2012 |
| Suzuki R, Saito K, Kato T, Shirakura M, Akazawa D, Ishii K, Aizaki H, Kanegae Y, Matsuura Y, Saito I, Wakita T, Suzuki T. | Trans-complemented hepatitis C virus particles as a versatile tool for study of virus assembly and infection. | Virology | 10 | 29-38 | 2012 |
| Murayama A, Sugiyama N, Watashi K, Masaki T, Suzuki R, Aizaki H, Mizuochi T, Wakita T, Kato T. | Japanese reference panel of blood specimens for evaluation of hepatitis C virus RNA and core antigen quantitative assays. | J Clin Microbiol | 50 | 1943-1949 | 2012 |
| Ando T, Imamura H, Suzuki R, Aizaki H, Watanabe T, Wakita T, Suzuki T. | Visualization and Measurement of ATP Levels in Living Cells Replicating Hepatitis C Virus Genome RNA. | PLOS Pathogen | 8 | e1002561 | 2012 |
| Moujalled DM, Cook WD, Okamoto T, Murphy J, Lawlor KE, Vince JE, Vaux DL. | TNF can activate RIPK3 and cause programmed necrosis in the absence of RIPK1. | Cell Death Dis. | 17 | e465 | 2013 |
| Okamoto T, Zobel K, Fedorova A, Quan C, Yang H, Fairbrother WJ, Huang DC, Smith BJ, Deshayes K, Czabotar PE. | Stabilizing the Pro-Apoptotic BimBH3 Helix (BimSAHB) Does Not Necessarily Enhance Affinity or Biological Activity. | ACS Chem Biol. | | [印刷中] | 2012 |

| | | | | | |
|---|---|---|---|---|---|
| Katoh H, Okamoto T, Fukuhara T, Kambara H, Morita E, Mori Y, Kamitani W, Matsuura Y. | Japanese Encephalitis Virus Core Protein Inhibits Stress Granule Formation through an Interaction with Caprin-1 and Facilitates Viral Propagation. | J.Virol. | 87 | 489-502 | 2012 |
| Giam M, Okamoto T, Mintern JD, Strasser A, Bouillet P | Bcl-2 family member Bcl-G is not a proapoptotic protein | Cell Death Dis. | 11 | e404. | 2012 |
| Okamoto T, Campbell S, Mehta N, Thibault J, Colman PM, Barry M, Huang DC, Kvansakul M. | Sheeppox Virus SPPV14 Encodes a Bcl-2-Like Cell Death Inhibitor That Counters a Distinct Set of Mammalian Proapoptotic Proteins. | J.Virol. | 86 | 11501-11511 | 2012 |
| Yamamoto M, Okuyama M, Ma JS, Kimura T, Kamiyama N, Saiga H, Ohshima J, Sasai M, Kayama H, Okamoto T, Huang DC, Soldati-Favre D, Horie K, Takeda J, Takeda K | A cluster of interferon-γ-inducible p65 GTPases plays a critical role in host defense against Toxoplasma gondii. | Immunity | 37 | 302-312 | 2012 |
| Komase K, Maekawa S, Miura M, Sueki R, Kadokura M, Shindo H, Shindo K, Amemiya F, Nakayama Y, Inoue T, Sakamoto M, Yamashita A, Moriishi K, Enomoto N. | serum RANTES level influences the response to pegylated-interferon and ribavirin therapy in chronic hepatitis C. | Hepatol Res. | (in press) | | 2012 |
| Sueki R, Maekawa S, Miura M, Kadokura M, Komase K, Shindo H, Kanayama A, Ohmori T, Shindo K, Amemiya F, Nakayama Y, Uetake T, Inoue T, Sakamoto M, Enomoto N. | Correlation between pretreatment viral sequences and the emergence of lamivudine resistance in hepatitis B virus infection. | J Med Virol. | 84(9) | 1360-8. | 2012 |

| | | | | | |
|---|---|---|---|---|---|
| Fujimoto Y, Salam KA,Furuta A, Matsuda Y, Fujita O, Tani H, Ikeda M, Kato N, Sakamoto N, Maekawa S, Enomoto N, de Voogd NJ, Nakakoshi M, Tsubuki M, Sekiguchi Y, Tsuneda S, Akimitsu N, Noda N, Yamashita A, Tanaka J, Moriishi K. | Inhibition of Both Protease and Helicase Activities of Hepatitis C Virus NS3 by an Ethyl Acetate Extract of Marine Sponge Amphimedon sp. | PLoS One. | 7(11) | e48685. | 2012 |
| Shindo H, Maekawa S, Komase K, Miura M, Kadokura M, Sueki R, Komatsu N, Shindo K, Amemiya F, Nakayama Y,Inoue T, Sakamoto M, Yamashita A, Moriishi K, Enomoto N. | IL-28B (IFN-λ3) and IFN- a synergistically inhibit HCV replication. | J Viral Hepatitis. | (in press) | | 2012 |
| Maekawa S, Sakamoto M, Miura M, Kadokura M, Sueki R, Komase K, Shindo H, Komatsu N, Shindo K, Kanayama A, Ohmori T, Amemiya F, Takano S, Yamaguchi T, Nakayama Y, Kitamura T, Inoue T, Okada S, Enomoto N. | Comprehensive analysis for viral elements and IL28B polymorphisms in response to peginterferon plus ribavirin therapy in hcv-1b infection. | Hepatology. | 56(5) | 1611-201221 | 2012 |
| Yamashita A, Salam KA, Furuta A, Matsuda Y, Fujita O, Tani H, Fujita Y, Fujimoto Y, Ikeda M, Kato N, Sakamoto N, Maekawa S, Enomoto N, Nakakoshi M, Tsubuki M, Sekiguchi Y, Tsuneda S, Akimitsu N, Noda N, Tanaka J, Moriishi K. | Inhibition of hepatitis C virus replication and viral helicase by ethyl acetate extract of the marine feather star Alloeocomatella polycladia. | Mar Drugs. | 10(4) | 744-61. | 2012 |

| | | | | | |
|---|---|---|---|---|---|
| Ordonez P, Hamasaki T,Isono Y, Sakakibara N,Ikejiri M, Maruyama T, Baba M | Anti-human immunodeficiency virus type 1 activity of novel 6-substituted 1-benzyl-3-(3,5-dimethylbenzyl)uracil derivatives. | Antimicrobial Agents and Chemotherapy | 56 巻 5 号 | 2581−1589 | 2012 年 |
| Thiyagarajan A,Salim MTA, Balaraju T, Bal C, Baba M, Sharon A. | Structure based medicinal chemistry approach to develop 4-methyl-7-deazaadenine carbocyclic nucleosides as anti-HCV agent. | Bioorganic Medicinal Chemistry Letters | 22 巻 24 号 | 7742−7747 | 2012 年 |
| Akbar SM, Chen S, Al-Mahtab M, Abe M, Hiasa Y, Onji M | Strong and multi-antigen specific immunity by hepatitis B core antigen (HBcAg)-based vaccines in a murine model of chronic hepatitis B: HBcAg is a candidate for a therapeutic vaccine against hepatitis B virus | Antiviral Res | 96 (1) | 59-64 | 2012 |
| Akbar SM, Hiasa Y, Al-Mahtab M, Onji M. | Dendritic cell-based immune therapy in liver diseases | Current Immunology Review | 8(1) | 28-36 | 2012 |
| Al-Mahtab M, Akbar SM, Rahman S, Kamal M, Khan MSI. | Biochemical, virological, immunological and histopathological features of 702 incidentally detected chronic hepatitis B virus carriers in Bangladesh | Digestion | 86(1) | 1-5 | 2012 |
| Hoshino H, Hino K, Miyakawa H, Takahashi K, Akbar SM, Mishiro S. | Inter-genotypic recombinant hepatitis C virus strains in Japan noticed by discrepancies between immunoassay and sequencing. | J Med Virol | 84(7) | 1018-1024 | 2012 |

| | | | | | |
|---|---|---|---|---|---|
| Miyashita K, Kang J-H, Saga A, Takahashi K, Shimamura T, Yasumoto A, Fukushima H, Sogabe S, Konishi K, Uchida K, Fujinaga A, Matsui T, Sakura Y, Tsuji T, Maguchi H, Taniguchi M, Abe N, Akbar SM, Arai M, Mishiro S | Three Cases of Acute or Fulminant Hepatitis E Caused by Ingestion of Pork Meat and Entrails in Hokkaido, Japan; Zoonotic Food-Borne Transmission of Hepatitis E Virus and Public Health Concerns. | Hepatol Res | 42(9) | 870-878. | 2012 |
| Date T, Kato T, Kato J, Takahashi H, Morikawa K, Akazawa D, Murayama A, Tanaka-Kaneko K, Sata T, Tanaka Y, Mizokami M, Wakita T. | Novel cell culture-adapted genotype 2a hepatitis C virus infectious clone. | J Virol. | 86(19) | 10805-20. | 2012 |
| Inokuchi M, Ito T, Nozawa H, Miyashita M, Morikawa K, Uchikoshi M, Shimozuma Y, Arai J, Shimazaki T, Hiroishi K, Imawari M. | Lymphotropic hepatitis C virus has an interferon-resistant phenotype. | J Viral Hepat. | 19(4) | 254-62. | 2012 |
| Date T, Morikawa K, Tanaka Y, Tanaka-Kaneko K, Sata T, Mizokami M, Wakita T. | Replication and infectivity of a novel genotype 1b hepatitis C virus clone. | Microbiol Immunol. | 56(5) | 308-17. | 2012 |
| Lange CM, Kutalik Z, Morikawa K, Bibert S, Cerny A, Dollenmaier G, Dufour JF, Gerlach TJ, Heim MH, Malinverni R, Müllhaupt B, Negro F, Moradpour D, Bochud PY; Swiss Hepatitis C Cohort Study Group. | Serum ferritin levels are associated with a distinct phenotype of chronic hepatitis C poorly responding to pegylated interferon-alpha and ribavirin therapy. | Hepatology. | 55(4) | 1038-47. | 2012 |

# Ⅳ．研究成果の刊行物・別冊

JVI
Journals.ASM.org

# Pin1 Interacts with the Epstein-Barr Virus DNA Polymerase Catalytic Subunit and Regulates Viral DNA Replication

**Yohei Narita,[a,c] Takayuki Murata,[a] Akihide Ryo,[b] Daisuke Kawashima,[a] Atsuko Sugimoto,[a,c] Teru Kanda,[a] Hiroshi Kimura,[c] Tatsuya Tsurumi[a]**

Division of Virology, Aichi Cancer Center Research Institute, Chikusa-ku, Nagoya,[a] Department of Microbiology, Yokohama City University School of Medicine, Kanazawa-ku, Yokohama,[b] Department of Virology, Nagoya University Graduate School of Medicine, Showa-ku, Nagoya,[c] Japan

**Peptidyl-prolyl *cis-trans* isomerase NIMA-interacting 1 (Pin1) protein is known as a regulator which recognizes phosphorylated Ser/Thr-Pro motifs and increases the rate of *cis* and *trans* amide isomer interconversion, thereby altering the conformation of its substrates. We found that Pin1 knockdown using short hairpin RNA (shRNA) technology resulted in strong suppression of productive Epstein-Barr virus (EBV) DNA replication. We further identified the EBV DNA polymerase catalytic subunit, BALF5, as a Pin1 substrate in glutathione *S*-transferase (GST) pulldown and immunoprecipitation assays. Lambda protein phosphatase treatment abolished the binding of BALF5 to Pin1, and mutation analysis of BALF5 revealed that replacement of the Thr178 residue by Ala (BALF5 T178A) disrupted the interaction with Pin1. To further test the effects of Pin1 in the context of virus infection, we constructed a BALF5-deficient recombinant virus. Exogenous supply of wild-type BALF5 in HEK293 cells with knockout recombinant EBV allowed efficient synthesis of viral genome DNA, but BALF5 T178A could not provide support as efficiently as wild-type BALF5. In conclusion, we found that EBV DNA polymerase BALF5 subunit interacts with Pin1 through BALF5 Thr178 in a phosphorylation-dependent manner. Pin1 might modulate EBV DNA polymerase conformation for efficient, productive viral DNA replication.**

The Epstein-Barr virus (EBV) is a human gammaherpesvirus that mainly infects and establishes latent infection in B lymphocytes, but it also can infect other types of cells, such as NK, T, and epithelial cells.

EBV has both a latent state and a lytic replicative cycle in the nuclei of EBV-infected cells (1). During the latent phase of the EBV life cycle, the EBV genome is maintained as a circular plasmid molecule, which is amplified once in S phase by cellular DNA replication machinery. However, a small percentage of infected cells switch from the latent stage into the lytic cycle, which is triggered by the expression of an immediate-early protein, BZLF1, to produce progeny viruses. This type of activation contributes to the development and maintenance of human cancers (2, 3), suggesting that the EBV switching mechanism is also a key determinant of EBV pathogenesis. After induction of productive viral replication, the EBV genome is amplified 100- to 1,000-fold by viral replication machinery composed of BALF5 DNA polymerase (Pol), BMRF1 polymerase processivity factor, BALF2 single-stranded DNA-binding protein, and BBLF4-BSLF1-BBLF2/BBLF3 (BBLF2/3) helicase-primase complex via a rolling-circle mechanism in discrete sites in nuclei, called replication compartments (4, 5). BALF5 possesses intrinsic DNA polymerase and 3′-to-5′ exonuclease activities (6) and forms a complex with the BMRF1 polymerase accessory protein to exhibit high polymerase processivity (7). The DNA polymerase and exonuclease domains are highly conserved among a variety of DNA polymerases (8, 9). Unlike the case of the eukaryotic chromosomal replication apparatus, the EBV DNA Pol holoenzyme is used in the synthesis of both leading and lagging strands at the replication fork (6).

The peptidyl-prolyl bond has a low rate of spontaneous *cis-trans* isomerization. This is frequently a limiting step for protein folding and usually requires an isomerase to catalyze the process. Phosphorylation on a serine or threonine residue preceding proline (pSer/Thr-Pro) is a key regulatory mechanism, and the conformation of certain phosphorylated Ser/Thr-Pro bonds is regulated specifically by the prolyl isomerase Pin1 (10). The WW domain of Pin1 binds only to specific pSer/Thr-Pro motifs, which are isomerized by the peptidyl-prolyl isomerase (PPIase) domain to induce conformational changes in proteins (11). In this way Pin1 regulates various protein functions, including protein stability, catalytic activity, phosphorylation status, protein-protein interactions, and/or subcellular localization (11–14). Pin1 works in concert with protein kinases that phosphorylate Ser/Thr-Pro motifs, and protein phosphatases, in turn, can also be regulators of the process (15). Pin1 has a pivotal role in a variety of biological processes such as cell cycle control (16), and its deregulation contributes to various pathological conditions, most notably cancer (11, 12, 17, 18). Pin1 is overexpressed in various human cancers, contributing to centrosome amplification, chromosome instability, and tumor development *in vitro* and *in vivo* and correlating with poor clinical outcomes (10, 19–22). In contrast, inhibition of Pin1 suppresses tumorigenesis *in vitro* (23) and prevents cancer development induced by overexpression of oncogenes such as Neu or Ras (24) or by knockout of tumor suppressors such as p53 (25) in mice.

Thus, Pin1 has key roles in control of cellular functions. However, its significance for EBV replication has yet to be clarified in detail. In this study, we show that Pin1 interacts with EBV DNA polymerase BALF5 and modulates productive viral DNA replica-

**Received** 25 September 2012 **Accepted** 27 November 2012
**Published ahead of print** 5 December 2012
Address correspondence to Tatsuya Tsurumi, ttsurumi@aichi-cc.jp, or Takayuki Murata, tmurata@aichi-cc.jp.

doi:10.1128/JVI.02634-12

tion. Because there is a very limited number of anti-EBV drugs developed or being developed to date, including acyclic nucleoside analogs, such as acyclovir, and kinase inhibitors, such as maribavir (26, 27), a search for an effective molecular target has been needed. Pin1 may be a potential target for development of novel antiviral drugs.

## MATERIALS AND METHODS

**Cell culture and reagents.** HEK293T and HEK293 EBV-bacterial artificial chromosome (BAC) cells were maintained in Dulbecco's modified Eagle's medium (Sigma) supplemented with 10% fetal bovine serum. B95-8 cells and an EBV-negative cell clone derived from Akata cells [Akata(−)] were cultured in RPMI medium supplemented with 10% fetal bovine serum. To induce lytic EBV replication, tetradecanoyl phorbol acetate (TPA), A23187, and sodium butyrate were added to the culture medium at final concentrations of 20 ng/ml, 1 μM, and 5 mM, respectively.

**Antibodies.** Rabbit anti-BZLF1, -BMRF1, -BALF2, and -BALF5 antibodies were as reported previously (28). An anti-EBV EA-D-p52/50 (BMRF1 gene product) protein-specific mouse monoclonal antibody, clone R3, was purchased from Chemicon Inc. Anti-Pin1 (H-123 and G-8) and anti-α/β-tubulin (2148) antibodies were purchased from Santa Cruz Biotechnology, Inc., and Cell Signaling, respectively. Horseradish peroxidase (HRP)-linked goat antibodies to rabbit IgG were from Amersham Biosciences.

**shRNA and siRNA.** Knockdown of Pin1 with short hairpin (shRNA) was carried out as described previously (29). As a control, we targeted the luciferase gene (designated shluc). Oligonucleotide sequences for the Pin1 shRNA (shPin1) were 5′-GATCCGCCGAGTGTACTACTTCAATTCAA GAGATTGAAGTAGTACACTCGGCTTTTTTAT-3′ (shPin1 for) and 5′-CGATAAAAAAGCCGAGTGTACTACTTCAATCTCTTGAATTGA AGTAGTACACTCGGCG-3′ (shPin1 rev), and the sequence for shluc was as noted previously (29). Duplexes of 21-nucleotide small interfering RNAs (siRNAs) were synthesized and annealed (Gene Design, Inc.). The sense and antisense sequences of the duplex were 5′-GCCAUUUGAAGA CGCCUCGdTdT-3′ and 5′-CGAGGCGUCUUCAAAUGGCdTdT-3′ for Pin1 and 5′-GCAGAGCUGGUUUAGUGAAdTdT-3′ and 5′-UUCA CUAAACCAGCUCUGCdTdT-3′ for the control siRNA.

**Measurement of the viral genome by qRT-PCR.** Cells were harvested at the time indicated in the figure legends and lysed with 200 μl of PCR lysis buffer (10 mM Tris-HCl [pH 8.0], 1 mM EDTA, 0.001% Triton X-100, and 0.001% SDS). After treatment with 25 μg of proteinase K at 50°C for 2 h, samples were boiled at 95°C for 10 min. Quantitative real-time PCR (qRT-PCR) was performed in 10 μl of solution containing 1 μM each forward and reverse primer, 5 μl of FastStart Universal Probe Master (Rox) (containing 6-carboxy-X-rhodamine [ROX] dye; Roche Applied Science), 0.5 μl of eukaryotic 18S rRNA endogenous control (Applied Biosystems), and 1 μl of prepared sample DNA in PCR lysis buffer. The intensity of ROX dye was used to compensate for volume fluctuations among the tubes. PCR included 2 min at 50°C and 10 min at 95°C and then 40 cycles at 95°C for 15 s, followed by 1 min at 60°C. Immediately after the PCR, we carried out dissociation curve analysis and confirmed the specificity of each PCR product. A standard curve was constructed using serial dilutions of DNA and was used to quantify the amount of DNA. Primers and a probe for detection of the viral genome were designed using Primer Express (Applied Biosystems) within the BALF2-coding region. The sequences were as follows: 5′-GCCCGTCCG GTTGTCA-3′ (forward primer), 5′-AATATCTGGTTGTTGCCGTTG A-3′ (reverse primer), and 5′-FAM-CTGCCAGTGACCATCAACAAGT ACACGG-TAMRA-3′ (probe; where FAM is 6-carboxyfluorescein and TAMRA is tetramethyl rhodamine).

**GST pulldown assays.** For bacterial expression of glutathione *S*-transferase (GST)-tagged Pin1 (wild type [WT] or the W34A mutant), *Escherichia coli* strain DH5α was transformed with the pGEX expression vector for each protein (10). Expression of GST fusion proteins was induced by the addition of isopropyl-β-D-thiogalactopyranoside (IPTG; 0.5 mM), followed by incubation at 25°C for 4 h. GST pulldown assays were conducted as described previously (10). In brief, B95-8 or HEK293 cell proteins were lysed in GST lysis buffer at 4°C. After sonication and centrifugation (at 20,000 × *g* for 10 min at 4°C), the supernatant was preincubated with glutathione-Sepharose beads (GE Healthcare) for 30 min at 4°C. Afterwards, the supernatant was mixed with 50 μg of GST fusion protein and glutathione beads for 1 h at 4°C with rotation. The beads were then washed with GST lysis buffer five times and subjected to immunoblotting.

**Transfection and IP.** Cells were transfected with appropriate plasmids using Lipofectamine 2000 reagent (Invitrogen) or by electroporation using a Microporator (Disital Bio). The total amounts of plasmid DNAs were standardized by addition of an empty vector. For immunoprecipitation (IP), cells were solubilized in 200 μl of 0.5% Nonidet P-40 buffer (10 mM Tris-HCl [pH 7.5], 100 mM NaCl, 0.5% Nonidet P-40, and protease and phosphatase inhibitor mixture). Cell extracts were then diluted with 800 μl of lysis buffer and precleared with protein G-Sepharose (GE Healthcare). Supernatants were then mixed with protein G-Sepharose and antibody and then incubated at 4°C for 4 h with rotation. Immunocomplexes were washed five times with the same buffer. Samples were subjected to SDS-PAGE, followed by immunoblotting with the antibodies indicated in the figures and figure legends. We used TrueBlot anti-rabbit IgG HRP-conjugated antibodies (eBioscience) as the secondary antibody to eliminate the immunoglobulin heavy chain/light chain-specific band.

**BALF5 expression plasmid and mutagenesis.** The expression vector for BALF5 was made by inserting the BALF5 open reading frame into the EcoRI/HindIII site of pcDNA3.1 (Invitrogen). Mutant vectors were generated by a PCR-based method using the following primers: TTCCATGT CTACGACATACTC (BALF5Δ1 For), ACACTTGGGAATGAGACGC (BALF5Δ1 Rev), AAGGTCACGCGCCGTTCCATT (BALF5Δ2 For), GA GGACTGCAAACTCCACGTC (BALF5Δ2 Rev), AGAAGAGCACAGGC TAGCC (BALF5Δ3 For), TTGTAGAATCCGGACAGGGG (BALF5Δ3 Rev), CTTCGAGTCATCTACGGGGAC (BALF5Δ4 For), GATGGAGAG GCAGGGAAAG (BALF5Δ4 Rev), GCCCCCTGCCGGGTCTCGG (BALF5-T178A For), and CCTGCGGTCGAAGGTGCTGG (BALF5-T178A Rev). The DNA sequence of each vector was confirmed by DNA sequencing using the following primers: GCATCGTCATCAAGCTACTG (BALF5-1), AGCTCGAGTACGACTGTGAG (BALF5-2), CACATCTAC AGCATCAACCC (BALF5-3), GATCCGCGTGTTCTCCTGC (BALF5-4), CCTTCTTGGCTAGTCTGTTG (BALF5-5), and TCCTGCCTGATG CTGATTAC (BALF5-6).

**Genetic manipulation of EBV-BAC DNA.** EBV-BAC DNA was provided by W. Hammerschmidt (30). Homologous recombination was undertaken in *E. coli* as described previously (28, 29, 31) with the following oligonucleotide primers: 5′-TGTGTGAACGTGTTTGGGCAGCAGGCC TACTTCTACGCCAGCGCGCCTCAGGGTCTGGACGGCCTGGTG ATGATGGCGGGATC-3′ (Neo/stFor), 5′-CGCGTGGCATCCACGTTG GCCTCAAAGATCCGACACCCGTGCTTGTCTTGCCACGTGTCAGA AGAACTCGTCAAGAAGG-3′ (Neo/stRev), 5′-AAGCCCTCTGGACTT CCATG-3′ (Transfer vector For), and 5′-CATTGTCCAGGACAAAGCG G-3′ (Transfer vector Rev). Electroporation was performed using a Gene Pulser III (Bio-Rad), and purification of EBV-BAC DNA was achieved with NucleoBond Bac100 (Macherey-Nagel, Germany).

## RESULTS

**Productive EBV DNA replication is strongly suppressed by knockdown of Pin1.** To determine whether Pin1 might influence productive EBV replication, we first carried out knockdown experiments. In HEK293 EBV-BAC cells featuring EBV latent infection, Pin1 expression was suppressed by shRNA (shPin1) transduction (Fig. 1A). An shRNA against the luciferase gene served as the control. Cells were transfected with empty vector pcDNA3 or pBZLF1, an expression vector for BZLF1, the molecular switch from latent to lytic infection of EBV. After 24 h, levels of viral and cellular proteins were examined by immunoblotting (Fig. 1A). In the control HEK293 EBV-BAC shluc cells, BZLF1 transfection

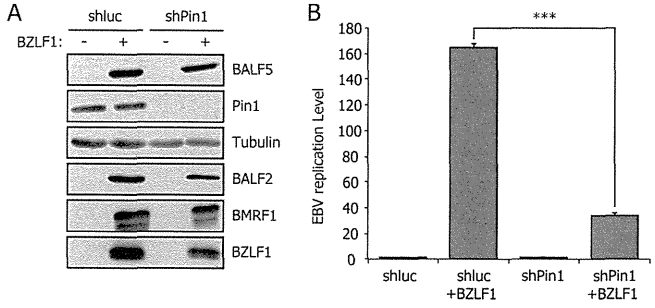


FIG 1 Knockdown of Pin1 decreases the level of EBV viral replication. (A) HEK293 EBV-BAC cells, transduced with control shRNA (shluc) or shRNA for Pin1 (shPin1), were transfected with 50 ng of BZLF1 expression vector or empty vector (pcDNA3). After 24 h, aliquots of cells were harvested and subjected to immunoblotting with the indicated antibodies. (B) Remaining cells transfected in panel A were subjected to qRT-PCR assays 60 h after transfection. The amount of EBV viral DNA was quantified and standardized with an 18S ribosome probe. Each bar represents the mean and standard deviation of three independent transfections and quantifications. ***, $P < 0.002$.

induced expression of viral genes such as BALF5, BALF2, and BMRF1, as expected, and knockdown of Pin1 (shPin1) had little effect on the expression levels.

We next checked the levels of viral DNA by qRT-PCR (Fig. 1B). The amount of synthesized EBV DNA was drastically and significantly reduced in Pin1-depleted cells upon induction compared to that in control cells, while levels of intrinsic, latent EBV genome copy numbers were comparable (Fig. 1B). Similar results were also obtained in lymphocytes (data not shown).

**Pin1 interacts with EBV DNA polymerase BALF5.** Since Pin1 was shown to contribute to EBV lytic replication (Fig. 1B), we next examined if certain EBV proteins could interact with Pin1 by GST pulldown assay. Whole-cell lysate from B95-8 cells treated with TPA-A23187-butyrate was incubated with purified GST-Pin1, GST-Pin1 W34A or GST alone expressed in bacteria. The W34A mutant of Pin1 served as a negative control because it cannot bind to the Ser/Thr-Pro motif of the substrates due to the mutation in its WW domain. We found that the viral DNA polymerase catalytic subunit, BALF5, was specifically and repeatedly coprecipitated with GST-Pin1 but not with GST alone or GST-Pin1 W34A

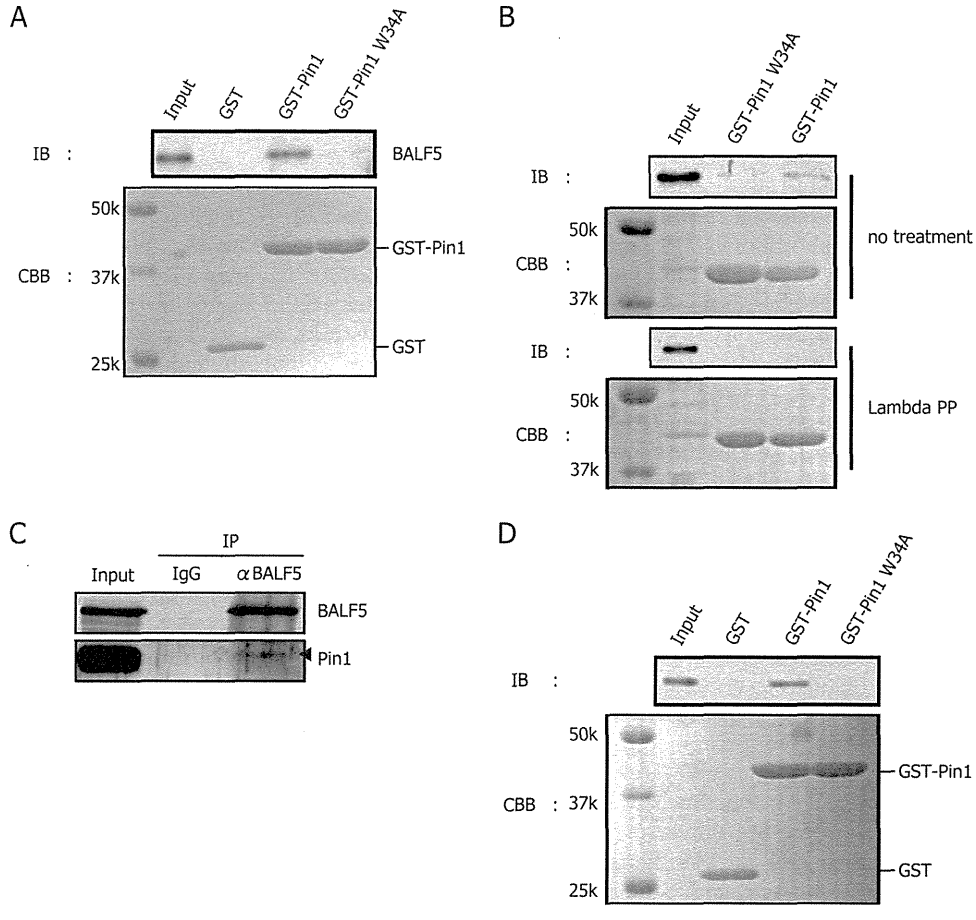


FIG 2 Pin1 interacts with EBV DNA polymerase BALF5. (A) GST-Pin1 binds to BALF5. Proteins from B95-8 cells, induced with TPA, A23187, and sodium butyrate for 24 h, were harvested and lysed in GST lysis buffer. GST pulldown assays were carried out using GST, GST-Pin1, or GST-Pin1 W34A. Pin1 W34A cannot bind with target proteins because of the mutation in its WW domain. (B) Phosphorylation-dependent association of Pin1. A GST pulldown assay was carried out as described for panel A except that the B95-8 cell lysate was incubated with lambda protein phosphatase (PP) (New England BioLabs) for 30 min at 30°C as indicated on the figure. (C) Immunoprecipitation assays confirmed the interaction. Cell proteins from lytic B95-8 lysate were subjected to immunoprecipitation using anti-BALF5 antibodies or normal IgG. The precipitates were then immunoblotted using anti-BALF5 or -Pin1 antibodies. α, anti. Arrowhead indicates size of Pin1. (D) Exogenously overexpressed BALF5 can bind to Pin1. Cell proteins from HEK293T cells transfected with BALF5 expression vector were subjected to GST pulldown assay. IB, immunoblotting; CBB, Coomassie brilliant blue. k, kilodaltons.

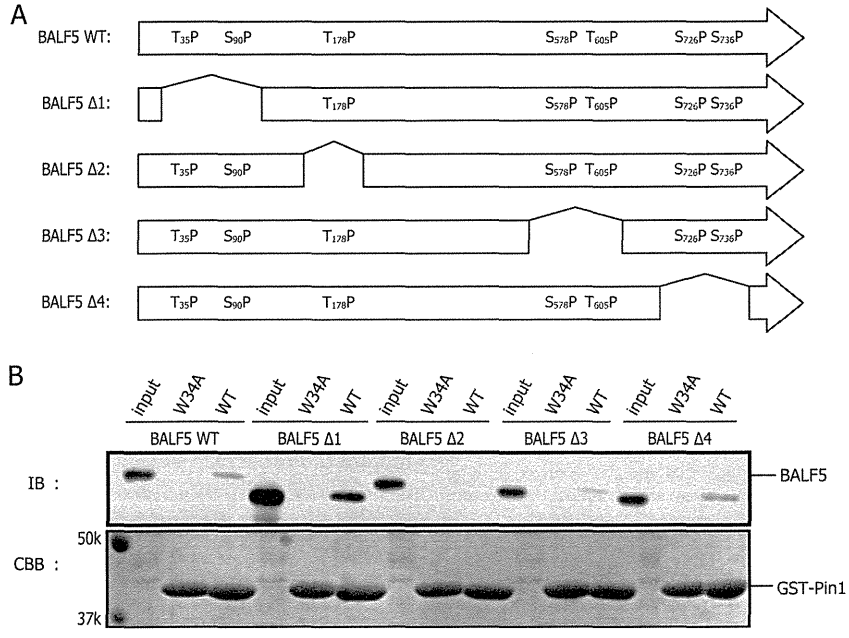


**FIG 3** Pin1 interacts with BALF5 Thr178. (A) Scheme of BALF5 truncated mutants, featuring deletion of amino acids 34 to 93 (BALF5Δ1), 167 to 185 (BALF5Δ2), 578 to 607 (BALF5Δ3), and 704 to 748 (BALF5Δ4). Primers used for constructing these mutants are listed in Materials and Methods. (B) Cell proteins lysed from HEK293T cells, transfected with the WT BALF5 expression vector or its derivatives shown in panel A, were subjected to GST pulldown assay.

(Fig. 2A). Other than BALF5, viral factors, such as BZLF1, BMRF1, BBLF4, BBLF2/3, and BSLF1, were not copurified with Pin1 in our GST pulldown assays (data not shown).

To test if the interaction was phosphorylation dependent, an aliquot of the lysate was treated with lambda phosphatase while the rest was left untreated (Fig. 2B). Dephosphorylation by the phosphatase diminished the interaction (Fig. 2B), suggesting that the two proteins associate in a phosphorylation-dependent manner (Fig. 2B).

Immunoprecipitation assays were next conducted in order to confirm the association between endogenous Pin1 and BALF5 in B95-8 cells. Pin1 was coimmunoprecipitated with BALF5, as expected (Fig. 2C).

For the experiments shown in Fig. 2A to C, we collected viral proteins from EBV-positive B95-8 cells after induction of lytic replication and demonstrated that Pin1 interacts with BALF5 in a phosphorylation-dependent manner. Since EBV encodes a protein kinase, BGLF4, we then examined whether phosphorylation of BALF5 by the viral kinase BGLF4 was necessary for the Pin1-BALF5 association. To this end, EBV-negative HEK293T cells were transfected with a expression vector plasmid for BALF5, and at 24 h posttransfection, GST pulldown assays were carried out using the lysate (Fig. 2D). Because the interaction between BALF5 and Pin1 was reproduced in an overexpression system, the viral kinase is apparently not a prerequisite for the interaction, and cellular kinases, such as mitogen-activated protein kinases (MAPKs) or cyclin-dependent kinases (CDKs), may be sufficient to mediate the association (17).

**Identification of the Ser/Thr-Pro motif in BALF5 required for association with Pin1.** Since phospho-Ser/Thr-Pro is the binding motif for Pin1, we searched for its presence in BALF5 protein. As shown in Fig. 3A (top panel), BALF5 has seven Ser/Thr-Pro motifs. In order to map the domain in BALF5 important for the interaction, we generated a series of BALF5 truncation mutants (Fig. 3A). There are four Ser-Pro (Ser90, Ser578, Ser726, and Ser736) and three Thr-Pro (Thr35, Thr178, and Thr605) motifs in the EBV BALF5 protein. We prepared mutants designated BALF5Δ1, BALF5Δ2, BALF5Δ3, and BALF5Δ4, featuring deletion of amino acids 34 to 93, 167 to 185, 578 to 607, and 704 to 748, respectively. HEK293T cells were transfected with BALF5 wild type (WT) or its mutants, and at 24 h posttransfection whole-cell extracts were subjected to GST pulldown assays. Among the truncation mutants, BALF5Δ2 exhibited attenuated association with GST-Pin1, whereas other mutants showed comparable binding ability with the wild type (Fig. 3B). As the truncated BALF5Δ2 mutant lacks BALF5 Thr178-Pro, the motif is suggested to be a potential candidate Pin1 binding site. Pulldown of BALF5Δ1 with GST-Pin1 appeared strong, but we believe the result was just an artifact simply because the input level of the protein was also high.

Considering BALF5 T178 as the Pin1 binding motif, we next constructed an alanine substitution mutant, designated BALF5 T178A. BALF5 WT or BALF5 T178A was expressed in HEK293T cells, and then cell lysates were subjected to GST pulldown assays (Fig. 4A). Levels of copurified BALF5 T178A with GST-Pin1 were markedly lower than with the wild type, as expected (Fig. 4A). Furthermore, immunoprecipitation assays also confirmed that the T178A mutation diminished the BALF5 association with Pin1 (Fig. 4B). Therefore, we conclude that BALF5 Thr178-Pro is the Pin1 binding target.

**BALF5 T178 is important for viral DNA polymerase activity.** Our experiments indicated only one Pin1 binding site in the BALF5 amino acid sequence. To further extend and verify the finding, recombinant EBV with BALF5 deletion was prepared. As shown in Fig. 5A, part of the BALF5 sequence encompassing the Pin1 binding site (Thr178) was replaced with a marker cassette (for neomycin resistance and streptomycin sensitivity [Neo/st]).

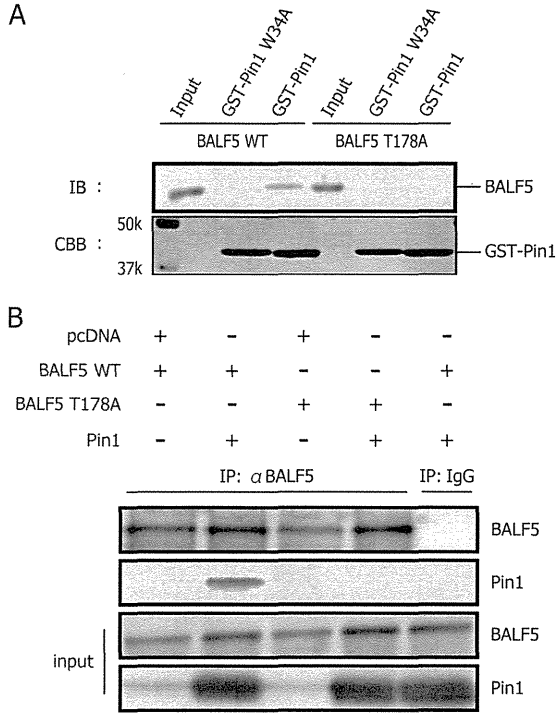


FIG 4 BALF5 T178A diminishes binding ability to Pin1. (A) Cell lysates from HEK293T cells, transfected with BALF5 wild type or T178A, were subjected to GST pulldown assays. (B) HEK293T cells were transfected with expression vectors for BALF5 wild type or T178A, with or without the expression vector for Pin1, as indicated. Cell proteins were lysed and subjected to immunoprecipitation using anti-BALF5 antibodies or normal IgG. The precipitates were then immunoblotted using anti-BALF5 or -Pin1 antibodies.

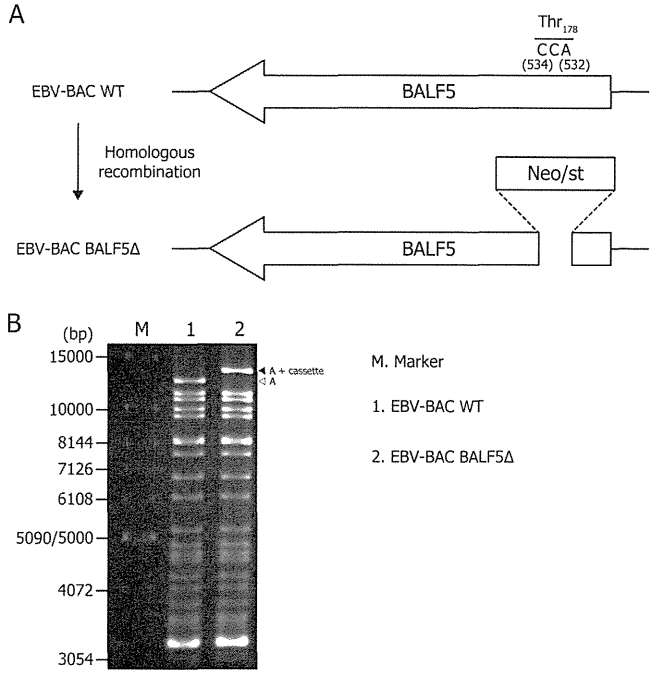


FIG 5 Scheme of EBV-BAC BALF5Δ construction. (A) Schematic arrangement of the recombination of the EBV genome using the neomycin-resistance and streptomycin-sensitivity genes (Neo/st) arranged in tandem. The sequence around the Pin1 binding site of BALF5 (Thr178) was replaced with the Neo/st cassette. (B) Electrophoresis of the recombinant viruses. The recombinant EBV genomes were digested with BamHI and separated in an agarose gel. A, the A fragment of BamHI-digested EBV-BAC.

Integrity of the BAC DNA was checked by BamHI digestion, followed by electrophoresis to confirm that the recombinant viruses did not carry obvious deletions or insertions. The BamHI-digested A fragment of EBV-BAC BALF5Δ (Fig. 5B, filled arrowhead) migrated more slowly than that of the wild type (open arrow), as expected, since the Neo/st marker cassette was inserted into the fragment (Fig. 5B).

Recombinant EBV-BAC DNA was introduced into a virus-producing cell line, HEK293, followed by hygromycin selection, to establish cell lines in which the EBV-BAC genome was maintained as an episome. More than 10 cell colonies from each recombinant virus were obtained, and viral protein expression levels in the presence and absence of BZLF1 induction were examined (data not shown). As the result, we obtained BALF5 knockout EBV-BAC cells (EBV-BAC BALF5Δ) which exhibited a typical nature, i.e., viral lytic protein expression was restricted without BZLF1 and efficiently induced by BZLF1.

In the BALF5 knockout cell line, exogenous expression of BZLF1 led to induction of early genes, such as BALF2 and BMRF1, but failed to produce BALF5, in line with expectations (Fig. 6A, BZLF1). Because of the lack of BALF5, the DNA Pol catalytic subunit, the virus could not amplify viral DNA even after induction with BZLF1 (Fig. 6C, BZLF1). Next, in order to compare the efficiencies of complementation, HEK293 EBV-BAC BALF5Δ cells were transfected with either BALF5 WT or BALF5 T178A expression vectors in addition to BZLF1. Exogenous supply of BALF5 WT restored the replication and increased viral DNA levels by 14.6-fold (Fig. 6C, BZLF1+BALF5 WT). On the other hand, the BALF5 T178A mutant increased the viral DNA only 4.54-fold (Fig. 6C, BZLF1+BALF5 T178A), when the mutant BALF5 protein expression level was equivalent to that of the wild type (Fig. 6A and B). In addition, we measured viral particles produced from the cells (Fig. 6D). Culture supernatant from the cells were collected and cocultured with naive Akata(−) cells. Since the recombinant EBVs used here encode green fluorescent protein (GFP), Akata(−) cells infected with EBV become GFP positive. When wild-type BALF5 was transfected with BZLF1, 759 infectious particles were obtained per ml of supernatant on average. Although the DNA replication levels (Fig. 6C) and viral yield (Fig. 6D) were slightly weak, we assume that this experimental condition is still physiologically relevant. The T178A mutation of BALF5 caused a slight decrease in the viral yield (Fig. 6D). These results indicate that the T178 residue of BALF5 is needed for efficient lytic replication of the EBV genome and suggest that optimal activity of the DNA polymerase is mediated through the interaction with Pin1.

To further verify the conclusion, we lastly tested if knockdown of Pin1 could influence EBV replication under this condition, too. Transfection of siRNA to HEK293 EBV-BAC BALF5Δ cells caused a considerable decrease in Pin1 levels when levels of other markers like BALF5, BZLF1, and tubulin remained unchanged (Fig. 6E). Viral replication levels this time reached 17.8-fold with BZLF1 plus BALF5 (wild type) and control siRNA, but Pin1 knockdown resulted in only a 12.2-fold increase (Fig. 6F). Although the difference in the results shown in Fig. 6F was less remarkable than the difference shown in Fig. 1B, we speculate that this reduction level by siPin1 is convincing enough because knockdown of Pin1 here

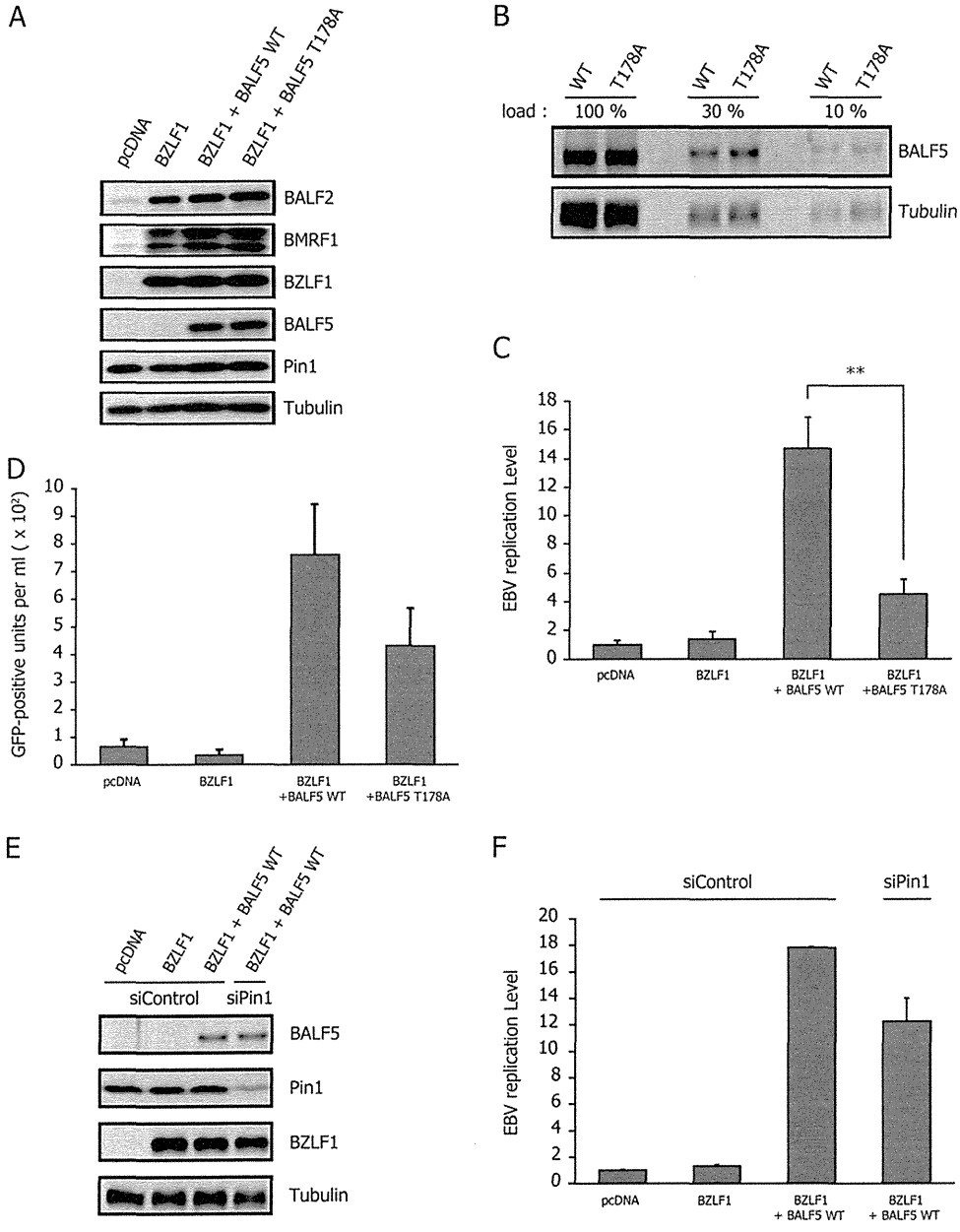


**FIG 6** Significance of Pin1 binding to BALF5 Thr178 for viral replication. (A) HEK293 EBV-BAC BALF5Δ cells were transfected with 50 ng of BZLF1 and 10 ng of either BALF5 WT or BALF5 T178A expression vector using a Microporator (Digital Bio). Aliquots of cells were harvested at 24 h after transfection and subjected to immunoblotting with indicated antibodies. (B) The samples from the third and fourth lanes of the experiment shown in panel A were diluted and loaded as indicated, followed by immunoblotting with anti-BALF5 and -tubulin antibodies. The remaining cells were harvested at 36 h after transfection and subjected to qRT-PCR (C). Each bar represents the mean and standard deviation for the viral DNA level after normalization, calculated from three independent samples. **, $P < 0.005$. (D) Culture supernatants from HEK293 EBV-BAC BALF5Δ cells, transfected in the same fashion as described for panel C and followed by 3 days of incubation, were collected and used to infect naive Akata(−) cells. Viral load in the medium was determined by fluorescence-activated cell sorting analysis and is shown as the number of GFP-positive units per milliliter. (E and F) HEK293 EBV-BAC BALF5Δ cells were transfected with siRNA against Pin1 (siPin1) or a control siRNA (siControl). After 2 days, the cells were then transfected with expression vectors for BZLF1, BALF5 WT, BALF5 T178A, and/or the empty vector pcDNA, as indicated. Samples were harvested at 24 h after transfection of plasmids and subjected to immunoblotting with the indicated antibodies (E). The remaining cells were harvested at 36 h after transfection of plasmids for qRT-PCR (F).

(Fig. 6E) was not as complete as that in the experiment shown in Fig. 1A.

## DISCUSSION

In this study, we obtained evidence for the first time of an interaction between the EBV lytic protein BALF5 and the cellular regulator Pin1. The results documented show clear involvement of the Pin1 protein in efficient EBV lytic replication. Initially, Pin1 was identified as a key regulator from knockdown experiments since silencing of Pin1 resulted in significant suppression of the viral replication level (Fig. 1).

We first speculated that knockdown of Pin1 might directly

influence viral lytic gene transcription because Pin1 reportedly regulates RNA polymerase II activity (32–34). Pin1 also impacts cellular signaling through factors such as Akt (35), c-Jun (36, 37), and p65/NF-κB (38). In fact, shPin1 might have slightly decreased EBV early gene expression (Fig. 1A) although we assume the levels are comparable.

Then, we found that the EBV DNA polymerase BALF5 interacted directly with Pin1, as demonstrated by GST pulldown (Fig. 2A), and that the interaction is dependent on phosphorylation of BALF5 Thr178 (Fig. 2B and 4). Results of immunoprecipitation assays also supported this conclusion (Fig. 2C and 4B). Although the association of Pin1 with BALF5 (Fig. 2 to 4) and its influence on viral DNA replication (Fig. 6) are clear, we cannot preclude the possibility that there may be other Pin1 substrates besides BALF5 that affect EBV genome amplification as Pin1 has a large number of substrates (12). Thus, the search for other Pin1 targets is still under way. In addition, it must also be noted that because there are a number of cellular target proteins that are up-/downregulated by Pin1, we cannot ignore the possibility that some of these cellular target proteins may cause even adverse effects on EBV replication. But as a whole, Pin1 clearly upregulates EBV lytic replication (Fig. 1), at least partly through the action of BALF5 (Fig. 6).

In this paper, we identified Pin1 interaction with the EBV DNA polymerase BALF5 enzyme at Thr178. The polymerase contains conserved domains, including polymerase catalytic and exonuclease domains at the C terminus, but the sequence around Thr178 is not conserved. We have no concrete idea of how Pin1 modulates BALF5 function, but it is possible that the N-terminal domain of BALF5, including Thr178, may somehow regulate its C-terminal functional domains by altering the structure of the protein in a subtle way. Further studies are required to gain an understanding of the molecular mechanism of how Pin1 regulates BALF5 enzymatic activity.

To our knowledge, EBV BALF5 is the only Pin1 target so far identified, not just in EBV but among all herpesvirus genes. Milbradt and others reported data suggesting that Pin1 may be involved in reorganization of nuclear lamin after phosphorylation by the human cytomegalovirus (HCMV)-encoded protein kinase UL97 (39). Elsewhere, Peloponese and others showed that Pin1 binds to the Tax protein of human T cell leukemia virus 1 and regulates Tax-induced NF-κB activation (40). Jeong and others demonstrated that Pin1 prolongs the Tax protein half-life by suppressing ubiquitination and proteasome-dependent degradation (41). Furthermore, Pin1 increased stability of the hepatitis B virus oncoprotein X and enhanced transactivation and cell proliferation (42). Hepatitis C virus replication is regulated by Pin1, probably through binding to NS5A/NS5B (43). Human immunodeficiency virus type 1 genome integration (44) and capsid uncoating (45) are also regulated by Pin1. Although exact roles of Pin1 in controlling herpesvirus replication remain elusive, it has already been proposed as an important modulator of viral proteins and a unique target for antiviral therapy (46).

A number of studies suggest that Pin1 has a role in tumorigenesis as it is overexpressed in a number of human cancers (47, 48). Since we determined that Pin1 is a positive regulator of EBV lytic replication, EBV-positive cancer tissue may be an efficient site for producing novel virus particles. While further studies are required to clarify the underlying mechanisms, Pin1 clearly warrants attention as a novel target for potential antiviral/cancer drug development.

## ACKNOWLEDGMENTS

We thank W. Hammerschmidt, H. J. Delecluse, and S. Tsuzuki for providing the EBV-BAC system, HEK293 cells, and shRNA technology, respectively. We also express our appreciation to C. Noda and T. Gamano for preliminary experiments and technical assistance.

This work was supported by grants-in-aid for Scientific Research from the Ministry of Education, Science, Sports, Culture and Technology (numbers 23390118 and 23114512 to T.T. and numbers 22790448 and 24590566 to T.M.), the Ministry of Health, Labor and Welfare (to T.T. and H.K.), and partly by the Takeda Science Foundation (to T.T. and T.M.).

## REFERENCES

1. **Tsurumi T, Fujita M, Kudoh A.** 2005. Latent and lytic Epstein-Barr virus replication strategies. Rev. Med. Virol. **15**:3–15.
2. **Feng WH, Cohen JI, Fischer S, Li L, Sneller M, Goldbach-Mansky R, Raab-Traub N, Delecluse HJ, Kenney SC.** 2004. Reactivation of latent Epstein-Barr virus by methotrexate: a potential contributor to methotrexate-associated lymphomas. J. Natl. Cancer Inst. **96**:1691–1702.
3. **Joab I, Nicolas JC, Schwaab G, de-The G, Clausse B, Perricaudet M, Zeng Y.** 1991. Detection of anti-Epstein-Barr-virus transactivator (ZEBRA) antibodies in sera from patients with nasopharyngeal carcinoma. Int. J. Cancer **48**:647–649.
4. **Daikoku T, Kudoh A, Fujita M, Sugaya Y, Isomura H, Shirata N, Tsurumi T.** 2005. Architecture of replication compartments formed during Epstein-Barr virus lytic replication. J. Virol. **79**:3409–3418.
5. **Fixman ED, Hayward GS, Hayward SD.** 1995. Replication of Epstein-Barr virus oriLyt: lack of a dedicated virally encoded origin-binding protein and dependence on Zta in cotransfection assays. J. Virol. **69**:2998–3006.
6. **Tsurumi T, Daikoku T, Nishiyama Y.** 1994. Further characterization of the interaction between the Epstein-Barr virus DNA polymerase catalytic subunit and its accessory subunit with regard to the 3′-to-5′ exonucleolytic activity and stability of initiation complex at primer terminus. J. Virol. **68**:3354–3363.
7. **Tsurumi T.** 1993. Purification and characterization of the DNA-binding activity of the Epstein-Barr virus DNA polymerase accessory protein BMRF1 gene products, as expressed in insect cells by using the baculovirus system. J. Virol. **67**:1681–1687.
8. **Bernad A, Blanco L, Lazaro JM, Martin G, Salas M.** 1989. A conserved 3′–5′ exonuclease active site in prokaryotic and eukaryotic DNA polymerases. Cell **59**:219–228.
9. **Bernad A, Zaballos A, Salas M, Blanco L.** 1987. Structural and functional relationships between prokaryotic and eukaryotic DNA polymerases. EMBO J. **6**:4219–4225.
10. **Ryo A, Nakamura M, Wulf G, Liou YC, Lu KP.** 2001. Pin1 regulates turnover and subcellular localization of beta-catenin by inhibiting its interaction with APC. Nat. Cell Biol. **3**:793–801.
11. **Lu KP, Zhou XZ.** 2007. The prolyl isomerase PIN1: a pivotal new twist in phosphorylation signalling and disease. Nat. Rev. Mol. Cell Biol. **8**:904–916.
12. **Liou YC, Zhou XZ, Lu KP.** 2011. Prolyl isomerase Pin1 as a molecular switch to determine the fate of phosphoproteins. Trends Biochem. Sci. **36**:501–514.
13. **Nakamura K, Greenwood A, Binder L, Bigio EH, Denial S, Nicholson L, Zhou XZ, Lu KP.** 2012. Proline isomer-specific antibodies reveal the early pathogenic tau conformation in Alzheimer's disease. Cell **149**:232–244.
14. **Wulf G, Finn G, Suizu F, Lu KP.** 2005. Phosphorylation-specific prolyl isomerization: is there an underlying theme? Nat. Cell Biol. **7**:435–441.
15. **Yeh ES, Means AR.** 2007. PIN1, the cell cycle and cancer. Nat. Rev. Cancer **7**:381–388.
16. **Winkler KE, Swenson KI, Kornbluth S, Means AR.** 2000. Requirement of the prolyl isomerase Pin1 for the replication checkpoint. Science **287**:1644–1647.
17. **Lu KP.** 2004. Pinning down cell signaling, cancer and Alzheimer's disease. Trends Biochem. Sci. **29**:200–209.

18. **Tun-Kyi A, Finn G, Greenwood A, Nowak M, Lee TH, Asara JM, Tsokos GC, Fitzgerald K, Israel E, Li X, Exley M, Nicholson LK, Lu KP.** 2011. Essential role for the prolyl isomerase Pin1 in Toll-like receptor signaling and type I interferon-mediated immunity. Nat. Immunol. **12**: 733–741.
19. **Ayala G, Wang D, Wulf G, Frolov A, Li R, Sowadski J, Wheeler TM, Lu KP, Bao L.** 2003. The prolyl isomerase Pin1 is a novel prognostic marker in human prostate cancer. Cancer Res. **63**:6244–6251.
20. **Bao L, Kimzey A, Sauter G, Sowadski JM, Lu KP, Wang DG.** 2004. Prevalent overexpression of prolyl isomerase Pin1 in human cancers. Am. J. Pathol. **164**:1727–1737.
21. **Lee KY, Lee JW, Nam HJ, Shim JH, Song Y, Kang KW.** 2011. PI3-kinase/p38 kinase-dependent E2F1 activation is critical for Pin1 induction in tamoxifen-resistant breast cancer cells. Mol. Cells **32**:107–111.
22. **Suizu F, Ryo A, Wulf G, Lim J, Lu KP.** 2006. Pin1 regulates centrosome duplication, and its overexpression induces centrosome amplification, chromosome instability, and oncogenesis. Mol. Cell. Biol. **26**:1463–1479.
23. **Ryo A, Liou YC, Wulf G, Nakamura M, Lee SW, Lu KP.** 2002. PIN1 is an E2F target gene essential for Neu/Ras-induced transformation of mammary epithelial cells. Mol. Cell. Biol. **22**:5281–5295.
24. **Wulf G, Garg P, Liou YC, Iglehart D, Lu KP.** 2004. Modeling breast cancer in vivo and ex vivo reveals an essential role of Pin1 in tumorigenesis. EMBO J. **23**:3397–3407.
25. **Takahashi K, Akiyama H, Shimazaki K, Uchida C, Akiyama-Okunuki H, Tomita M, Fukumoto M, Uchida T.** 2007. Ablation of a peptidyl prolyl isomerase Pin1 from p53-null mice accelerated thymic hyperplasia by increasing the level of the intracellular form of Notch1. Oncogene **26**: 3835–3845.
26. **Gershburg E, Hong K, Pagano JS.** 2004. Effects of maribavir and selected indolocarbazoles on Epstein-Barr virus protein kinase BGLF4 and on viral lytic replication. Antimicrob. Agents Chemother. **48**:1900–1903.
27. **Wang FZ, Roy D, Gershburg E, Whitehurst CB, Dittmer DP, Pagano JS.** 2009. Maribavir inhibits Epstein-Barr virus transcription in addition to viral DNA replication. J. Virol. **83**:12108–12117.
28. **Murata T, Isomura H, Yamashita Y, Toyama S, Sato Y, Nakayama S, Kudoh A, Iwahori S, Kanda T, Tsurumi T.** 2009. Efficient production of infectious viruses requires enzymatic activity of Epstein-Barr virus protein kinase. Virology **389**:75–81.
29. **Noda C, Murata T, Kanda T, Yoshiyama H, Sugimoto A, Kawashima D, Saito S, Isomura H, Tsurumi T.** 2011. Identification and characterization of CCAAT enhancer-binding protein (C/EBP) as a transcriptional activator for Epstein-Barr virus oncogene latent membrane protein 1. J. Biol. Chem. **286**:42524–42533.
30. **Delecluse HJ, Hilsendegen T, Pich D, Zeidler R, Hammerschmidt W.** 1998. Propagation and recovery of intact, infectious Epstein-Barr virus from prokaryotic to human cells. Proc. Natl. Acad. Sci. U. S. A. **95**:8245–8250.
31. **Isomura H, Stinski MF, Kudoh A, Murata T, Nakayama S, Sato Y, Iwahori S, Tsurumi T.** 2008. Noncanonical TATA sequence in the UL44 late promoter of human cytomegalovirus is required for the accumulation of late viral transcripts. J. Virol. **82**:1638–1646.
32. **Palancade B, Marshall NF, Tremeau-Bravard A, Bensaude O, Dahmus ME, Dubois MF.** 2004. Dephosphorylation of RNA polymerase II by CTD-phosphatase FCP1 is inhibited by phospho-CTD associating proteins. J. Mol. Biol. **335**:415–424.
33. **Xu YX, Hirose Y, Zhou XZ, Lu KP, Manley JL.** 2003. Pin1 modulates the structure and function of human RNA polymerase II. Genes Dev. **17**: 2765–2776.
34. **Xu YX, Manley JL.** 2007. Pin1 modulates RNA polymerase II activity during the transcription cycle. Genes Dev. **21**:2950–2962.
35. **Liao Y, Wei Y, Zhou X, Yang JY, Dai C, Chen YJ, Agarwal NK, Sarbassov D, Shi D, Yu D, Hung MC.** 2009. Peptidyl-prolyl *cis/trans* isomerase Pin1 is critical for the regulation of PKB/Akt stability and activation phosphorylation. Oncogene **28**:2436–2445.
36. **Pulikkan JA, Dengler V, Peer Zada AA, Kawasaki A, Geletu M, Pasalic Z, Bohlander SK, Ryo A, Tenen DG, Behre G.** 2010. Elevated PIN1 expression by C/EBPα-p30 blocks C/EBPα-induced granulocytic differentiation through c-Jun in AML. Leukemia **24**:914–923.
37. **Wulf GM, Ryo A, Wulf GG, Lee SW, Niu T, Petkova V, Lu KP.** 2001. Pin1 is overexpressed in breast cancer and cooperates with Ras signaling in increasing the transcriptional activity of c-Jun towards cyclin D1. EMBO J. **20**:3459–3472.
38. **Ryo A, Suizu F, Yoshida Y, Perrem K, Liou YC, Wulf G, Rottapel R, Yamaoka S, Lu KP.** 2003. Regulation of NF-κB signaling by Pin1-dependent prolyl isomerization and ubiquitin-mediated proteolysis of p65/RelA. Mol. Cell **12**:1413–1426.
39. **Milbradt J, Webel R, Auerochs S, Sticht H, Marschall M.** 2010. Novel mode of phosphorylation-triggered reorganization of the nuclear lamina during nuclear egress of human cytomegalovirus. J. Biol. Chem. **285**: 13979–13989.
40. **Peloponese JM, Jr, Yasunaga J, Kinjo T, Watashi K, Jeang KT.** 2009. Peptidylproline *cis-trans*-isomerase Pin1 interacts with human T-cell leukemia virus type 1 Tax and modulates its activation of NF-κB. J. Virol. **83**:3238–3248.
41. **Jeong SJ, Ryo A, Yamamoto N.** 2009. The prolyl isomerase Pin1 stabilizes the human T-cell leukemia virus type 1 (HTLV-1) Tax oncoprotein and promotes malignant transformation. Biochem. Biophys. Res. Commun. **381**:294–299.
42. **Pang R, Lee TK, Poon RT, Fan ST, Wong KB, Kwong YL, Tse E.** 2007. Pin1 interacts with a specific serine-proline motif of hepatitis B virus X-protein to enhance hepatocarcinogenesis. Gastroenterology **132**:1088–1103.
43. **Lim YS, Tran HT, Park SJ, Yim SA, Hwang SB.** 2011. Peptidyl-prolyl isomerase Pin1 is a cellular factor required for hepatitis C virus propagation. J. Virol. **85**:8777–8788.
44. **Manganaro L, Lusic M, Gutierrez MI, Cereseto A, Del Sal G, Giacca M.** 2010. Concerted action of cellular JNK and Pin1 restricts HIV-1 genome integration to activated $CD4^+$ T lymphocytes. Nat. Med. **16**:329–333.
45. **Misumi S, Inoue M, Dochi T, Kishimoto N, Hasegawa N, Takamune N, Shoji S.** 2010. Uncoating of human immunodeficiency virus type 1 requires prolyl isomerase Pin1. J. Biol. Chem. **285**:25185–25195.
46. **Kojima Y, Ryo A.** 2010. Pinning down viral proteins: a new prototype for virus-host cell interaction. Front. Microbiol. **1**:107. doi:10.3389/fmicb.2010.00107.
47. **Ryo A, Liou YC, Lu KP, Wulf G.** 2003. Prolyl isomerase Pin1: a catalyst for oncogenesis and a potential therapeutic target in cancer. J. Cell Sci. **116**:773–783.
48. **Ryo A, Uemura H, Ishiguro H, Saitoh T, Yamaguchi A, Perrem K, Kubota Y, Lu KP, Aoki I.** 2005. Stable suppression of tumorigenicity by Pin1-targeted RNA interference in prostate cancer. Clin. Cancer Res. **11**: 7523–7531.

VIROLOGY

# Interferon-Induced SCYL2 Limits Release of HIV-1 by Triggering PP2A-Mediated Dephosphorylation of the Viral Protein Vpu

Kei Miyakawa,[1,2] Tatsuya Sawasaki,[3] Satoko Matsunaga,[1] Andrey Tokarev,[4] Gary Quinn,[1] Hirokazu Kimura,[5] Masako Nomaguchi,[6] Akio Adachi,[6] Naoki Yamamoto,[7] John Guatelli,[4,8] Akihide Ryo[1]*

**Human cells respond to infection by retroviruses through the actions of proteins that inhibit the spread of viruses to other cells. One example is bone marrow stromal cell antigen 2 (BST2; also known as tetherin), which is an interferon (IFN)–inducible protein that restricts the release of progeny virions from infected cells. The HIV-1 accessory protein Vpu (viral protein U) causes degradation of BST2, and phosphorylation of Vpu at residues Ser$^{52}$ and Ser$^{56}$ is required for this function. We report that the host protein SCY1-like protein 2 (SCYL2) mediates the dephosphorylation of Vpu, antagonizing Vpu function and facilitating BST2-dependent restriction of HIV-1 release. SCYL2 reduced the number of virus particles released from cells infected with wild-type HIV-1, but not a strain lacking *vpu*, in a BST2-dependent manner. SCYL2 stimulated the dephosphorylation of Vpu on Ser$^{52}$ and Ser$^{56}$ by recruiting protein phosphatase 2A (PP2A) to Vpu. Conversely, depletion of SCYL2 resulted in enhanced phosphorylation of Vpu and increased viral particle release. Moreover, SCYL2 was produced in response to type I IFN and contributed to IFN-mediated viral restriction. Together, these results suggest that SCYL2 serves as a regulatory factor for Vpu, reducing the extent of Vpu phosphorylation and consequently enhancing BST2-mediated viral restriction.**

## INTRODUCTION

Accumulating evidence indicates that the HIV-1 accessory proteins antagonize host defenses to support efficient viral replication (*1*–*5*). Viral protein U (Vpu) is an 81–amino acid residue accessory protein that is encoded by HIV-1, simian immunodeficiency virus isolated from chimpanzees ($SIV_{CPZ}$), and some SIVs isolated from Old World monkeys (the $SIV_{GSN}$ lineage). Vpu is translated from a bicistronic mRNA that also encodes the viral envelope glycoprotein (Env) (*6*–*8*). Although Vpu is not absolutely required for HIV-1 replication (*6*), studies with molecular clones of virus lacking *vpu* have demonstrated that the Vpu protein substantially enhances the production of infectious virus through at least two distinct mechanisms: the proteasomal degradation of CD4 (*9*) and the functional inactivation of the interferon (IFN)–inducible restriction factor bone marrow stromal cell antigen 2 (BST2; also known as tetherin) (*10*, *11*).

Cell-surface CD4 acts as an entry receptor for HIV-1, but it also inhibits viral release and virion infectivity (*12*, *13*). CD4 binds to the Env precursor protein gp160 in the endoplasmic reticulum (ER) and inhibits its processing to gp120 and gp41. Vpu physically interacts with CD4 in the ER and facilitates its degradation, enabling Env processing and the efficient production of infectious virions (*14*). The restriction factor BST2 inhibits viral particle release, but similar to the effects of CD4, this inhibition is functionally counteracted by Vpu (*10*, *11*). Vpu reduces the cell-surface abundance of BST2 through transmembrane interactions (*11*, *15*–*21*), and it directs the degradation of BST2, primarily in lysosomes (*15*–*17*, *22*–*25*). In the absence of Vpu, BST2 cross-links nascent virions to the plasma membrane of infected cells and substantially inhibits the release of viral particles (*26*–*28*).

Previous reports indicated that Vpu is phosphorylated, presumably by casein kinase II (CKII), on two phospho-acceptor sites (Ser$^{52}$ and Ser$^{56}$) in its cytoplasmic domain (*29*, *30*). Phosphorylation of both residues is required for efficient Vpu-mediated removal of BST2 from the cell surface as well as for the degradation of CD4 (*15*, *23*, *24*, *31*, *32*). The amino acid sequence of the region of Vpu (DpS$^{52}$GxxpS$^{56}$) that contains both phosphorylated serines (pS) residues is recognized by an F-box–containing ubiquitin ligase subunit, β transducin repeat–containing protein (β-TrCP). Vpu thus recruits the multisubunit SCF (Skp1-Cullin-F-box)–β-TrCP E3 ubiquitin ligase complex, which leads to the ubiquitination and degradation of BST2 and CD4 (*15*, *23*, *24*, *33*). Indeed, an HIV-1 clone carrying a mutation in the β-TrCP–binding motif of Vpu fails to reduce BST2 abundance in infected T cells (*15*, *34*). Although the phosphorylation of Vpu on Ser$^{52}$ and Ser$^{56}$ is a crucial step in the Vpu-dependent inhibition of BST2, how this process is further regulated is not well understood.

The type I IFN system, which includes IFN-α and IFN-β, is an innate immune response to viral infection and creates an antiviral state in cells that provides an important first line of defense against viral infection (*35*). Type I IFN is widely believed to have an inhibitory effect on HIV-1 replication (*36*). The biological response to IFN is mediated by its binding to the IFN receptors and the activation of the Janus-activated kinase (JAK)–signal transducer and activator of transcription (STAT) pathway, which leads to the expression of several hundred IFN-stimulated genes (ISGs) (*37*). Although BST2 has been described as an ISG (*38*), Vpu targets

[1]Department of Microbiology, Yokohama City University School of Medicine, Kanagawa 236-0004, Japan. [2]Japanese Foundation for AIDS Prevention, Tokyo 101-0061, Japan. [3]Cell-Free Science and Technology Research Center, Ehime University, Ehime 790-8577, Japan. [4]Department of Medicine, University of California, La Jolla, CA 92093, USA. [5]Infectious Disease Surveillance Center, National Institute of Infectious Diseases, Tokyo 208-0011, Japan. [6]Department of Microbiology, Institute of Health Biosciences, The University of Tokushima Graduate School, Tokushima 770-8503, Japan. [7]Department of Microbiology, National University of Singapore, Singapore 117597, Singapore. [8]San Diego Veterans Affairs Healthcare System, San Diego, CA 92161, USA.
*To whom correspondence should be addressed. E-mail: aryo@yokohama-cu.ac.jp

IFN-induced BST2 for removal from the cell surface, which is the apparent site of action of BST2 as a restriction factor. This suggests that Vpu plays a major role in conferring resistance on the innate immune response. However, treatment of HIV-1–infected cells with type I IFN can suppress viral particle release even in the presence of Vpu (*39–41*). This finding prompted us to hypothesize that the function of Vpu could be modulated by other host factors that would likely be induced by type I IFN; however, no such factor has yet been identified. To identify host factors that regulate Vpu activity, we used an in vitro, high-throughput protein-protein interaction assay with full-length HIV-1 Vpu and host kinase–related proteins synthesized in the wheat cell-free protein production system. Here, we report that SCY1-like protein 2 (SCYL2) is a functional interactor of Vpu and that it inhibits Vpu function by promoting the dephosphorylation of Vpu by the phosphatase protein phosphatase 2A (PP2A).

## RESULTS

### SCYL2 is a Vpu-binding host protein

We initially conducted in vitro protein-protein interaction analysis with full-length HIV-1 Vpu and host proteins. Because Vpu phosphorylation is required for its function, we focused on human protein kinases and related proteins as potential Vpu regulators. We synthesized more than 400 host proteins with a wheat cell-free protein production system (*42*) and screened them for their association with Vpu with the amplified luminescent proximity homogeneous assay (AlphaScreen) (*43*, *44*) (Fig. 1, A and B, and fig. S1). When a relative light unit per cutoff ratio of ≥5000 was used as the threshold, we identified 13 host proteins as potential factors to interact with Vpu that had not been previously known to do so (Fig. 1C). Using gene ontology analysis, we eliminated nuclear proteins relevant to transcriptional regulation or meiosis, enabling us to focus on nine proteins for additional screening (Fig. 1C). To assess the roles of these host proteins in the context of viral replication, we conducted small interfering RNA (siRNA)–based functional analysis of virus particle production. We transfected HeLa cells (which express BST2 endogenously) with siRNAs targeting the nine selected host factors, and then we transfected the cells with an HIV-1 proviral plasmid (pNL4-3). Subsequent measurement of the concentrations of the HIV-1 capsid protein p24 in the culture media by enzyme-linked immunosorbent assay (ELISA) revealed that siRNA specific for SCYL2 caused a substantial increase in viral particle release (Fig. 1D). On the basis of this initial screening, we focused on SCYL2 as a previously uncharacterized Vpu-interacting factor for in-depth functional analysis.

### SCYL2 inhibits the particle release of Vpu-positive HIV-1

We next investigated whether SCYL2 affected viral particle release in the presence or absence of either BST2 or Vpu. We transfected HeLa cells with a wild-type or a Vpu-deficient HIV-1 molecular clone (pNL4-3 or pNL4-3ΔVpu) together with a plasmid encoding SCYL2. Viral release assays revealed that in HeLa cells expressing endogenous BST2, the presence of SCYL2 inhibited the release of wild-type HIV-1 particles and increased the amounts of intracellular BST2 (Fig. 2, A and B). Moreover, in cells transfected with pNL4-3ΔVpu, SCYL2 affected neither viral release nor intracellular BST2 abundance (Fig. 2, A and B). We further confirmed that SCYL2 had no observable suppressive effect on viral release in BST2-knockdown HeLa cells (Fig. 2C) or in human embryonic kidney (HEK) 293T cells, which lack endogenous BST2 (Fig. 2D). Moreover, the targeted depletion of endogenous SCYL2 substantially enhanced the release of wild-type virus, but not of Vpu-deficient virus, from cells containing BST2 (Fig. 2, E to G). Together, these results suggested that SCYL2 inhibited the release of viral particles only in the presence of BST2 and Vpu.

### SCYL2 inhibits the Vpu-induced reduction in BST2 abundance

Many reports have demonstrated that Vpu enhances viral release by removing BST2 from the cell surface (*11*, *15–20*). To examine whether SCYL2 affected this function of Vpu, we investigated the amounts of cell-surface

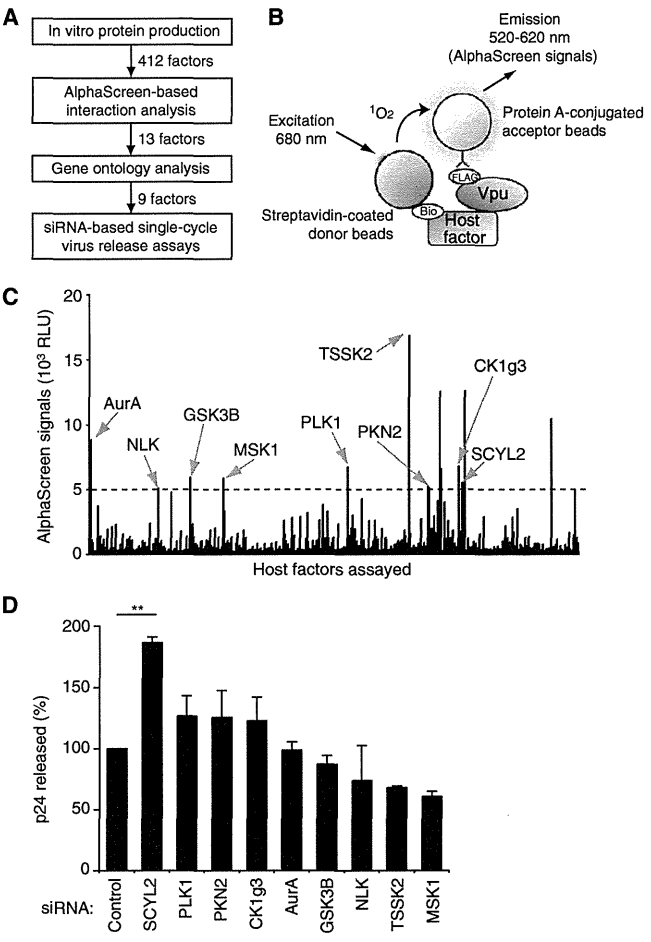


Fig. 1. SCYL2 is a Vpu-binding host protein. (**A**) Overview of the experimental procedure to detect regulatory factors for HIV-1 Vpu. (**B**) Schematic representation of the amplified luminescent proximity homogeneous assay used to identify Vpu-interacting proteins. Streptavidin-coated donor beads and anti-FLAG antibody conjugated to protein A acceptor beads were mixed with Vpu and human host proteins. If the two proteins are within 200 nm of each other, AlphaScreen signals are detected. (**C**) Thirteen proteins with high AlphaScreen signals were processed for further validation by gene ontology analysis. The nine kinases shown were selected as candidate Vpu-interacting host factors. The AlphaScreen was performed in duplicate for each sample. (**D**) An siRNA-based analysis measuring HIV-1 particle production. HeLa cells were treated with the indicated siRNAs for 24 hours before being transfected with the pNL4-3 molecular clone. Forty-eight hours after transfection, p24 protein in culture supernatants was measured by ELISA. $^{**}P = 0.0030$; $n = 3$ experiments.

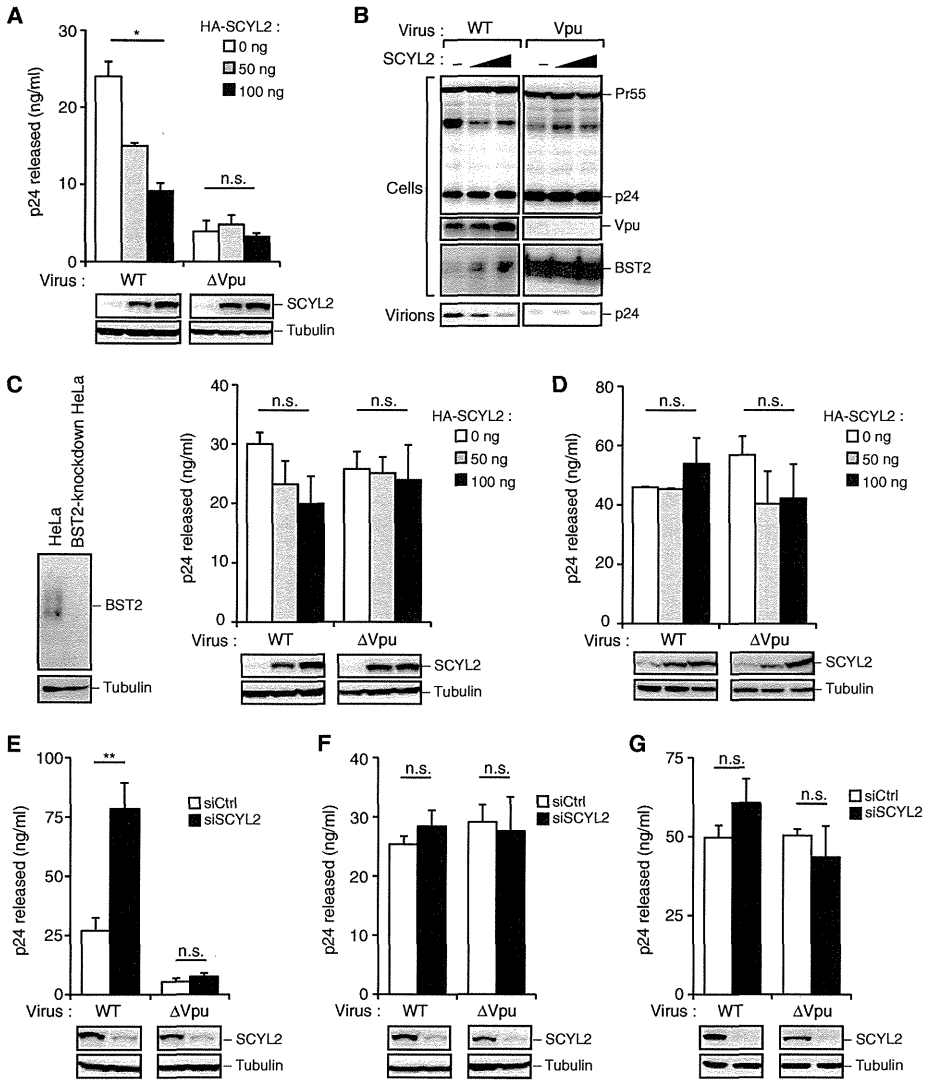


Fig. 2. SCYL2 inhibits the release of particles of Vpu-positive HIV-1. (A and B) Single-cycle virus release analysis of wild-type (WT) or Vpu-deficient HIV-$1_{NL4-3}$. HeLa cells were cotransfected with the indicated amounts of the SCYL2 expression plasmid together with 100 ng of either pNL4-3 (WT) or pNL4-3ΔVpu (ΔVpu). (A) Forty-eight hours after transfection, culture supernatants were analyzed by ELISA for p24 protein. Blots below the bar graph show the detection of SCYL2 and tubulin by Western blotting. n.s., not significant; *$P$ = 0.0206; $n$ = 3 experiments. (B) Cell lysates and supernatants were processed by Western blotting with antibodies against the indicated proteins. (C and D) SCYL2 fails to inhibit viral release from BST2-deficient cells. (C) BST2-knockdown HeLa cells and (D) HEK 293T cells (which have no endogenous BST2) were cotransfected with the indicated amounts of the SCYL2 expression plasmid together with 100 ng of either pNL4-3 or pNL4-3ΔVpu. Forty-eight hours after transfection, culture supernatants were analyzed by p24 ELISA. Western blotting analysis to detect BST2 abundance (C, left) and SCYL2 abundance (C and D, bottom) are shown. n.s., not significant; $n$ = 3 experiments. (E to G) SCYL2 depletion enhances viral release from cells containing BST2. Single-cycle virus release analysis of WT or Vpu-deficient HIV-$1_{NL4-3}$ in (E) HeLa cells, (F) BST2-knockdown HeLa cells, and (G) HEK 293T cells. Each cell type was treated with either control (white bars) or SCYL2-specific siRNAs (black bars) for 24 hours before being transfected with either pNL4-3 or pNL4-3ΔVpu (100 ng). Forty-eight hours after transfection, culture supernatants were analyzed by ELISA for p24. Western blotting analysis to detect endogenous SCYL2 abundance is shown at the bottom. n.s., not significant; **$P$ = 0.0023; $n$ = 3 experiments.

BST2 in HeLa cells expressing Vpu alone or in the presence of SCYL2. Consistent with previous studies, Vpu reduced the abundance of BST2 at the cell surface (Fig. 3A). However, this reduction was less apparent when cells were cotransfected with plasmids encoding both Vpu and SCYL2 (Fig. 3A). Western blotting analysis revealed that the presence of SCYL2 also inhibited the Vpu-mediated degradation of BST2 (Fig. 3B). We next addressed whether SCYL2 affected the anti-BST2 activity of Kaposi's sarcoma–associated herpesvirus (KSHV) K5 protein (*22*, *45*, *46*). Flow cytometric analysis demonstrated that SCYL2 was not able to revert the reduction in the cell-surface abundance of BST2 by KSHV K5 (Fig. 3C). Furthermore, SCYL2 inhibited the ability of Vpu to remove CD4 from the cell surface (Fig. 3D). These results indicated that SCYL2 specifically antagonized the function of Vpu and that this antagonism applied to the effects of Vpu on two cellular targets, CD4 and BST2.

## SCYL2 inhibits the phosphorylation of Vpu on $Ser^{52}$ and $Ser^{56}$

Vpu contains two conserved phosphoacceptor sites ($Ser^{52}$ and $Ser^{56}$) in its cytoplasmic domain. Phosphorylation of these residues by CKII is required for efficient Vpu function with respect to decreasing the abundances of both BST2 and CD4 (*15*, *23*, *24*, *31*, *32*). We thus speculated that SCYL2 might affect the phosphorylation status of Vpu at $Ser^{52}$ and $Ser^{56}$. To monitor the extent of Vpu phosphorylation in cells, we used phosphate-affinity polyacrylamide gel electrophoresis (Phos-tag PAGE) (*47*). This method enables the visualization of the phosphorylation status of a protein as a distinct band shift (*48*, *49*). In our Phos-tag PAGE analysis, wild-type Vpu was detected as an upper-shifted band, whereas a mutant Vpu in which $Ser^{52}$ and $Ser^{56}$ were replaced with alanines [Vpu(S52,56A)] was detected as a lower-shifted band, suggesting that the slower-migrating band was as a result of the phosphorylation of Vpu on $Ser^{52}$ and $Ser^{56}$ (Fig. 4A). SCYL2 converted wild-type Vpu into its dephosphorylated state (Fig. 4A). To confirm this observation, we generated a phospho-specific antibody against $Ser^{52}$ and $Ser^{56}$ of Vpu that detects wild-type Vpu but neither the Vpu(S52,56A) mutant nor calf intestinal phosphatase–treated wild-type Vpu (Fig. 4B). We used this antibody for Western blotting analysis and found, as expected, that SCYL2 reduced the extent

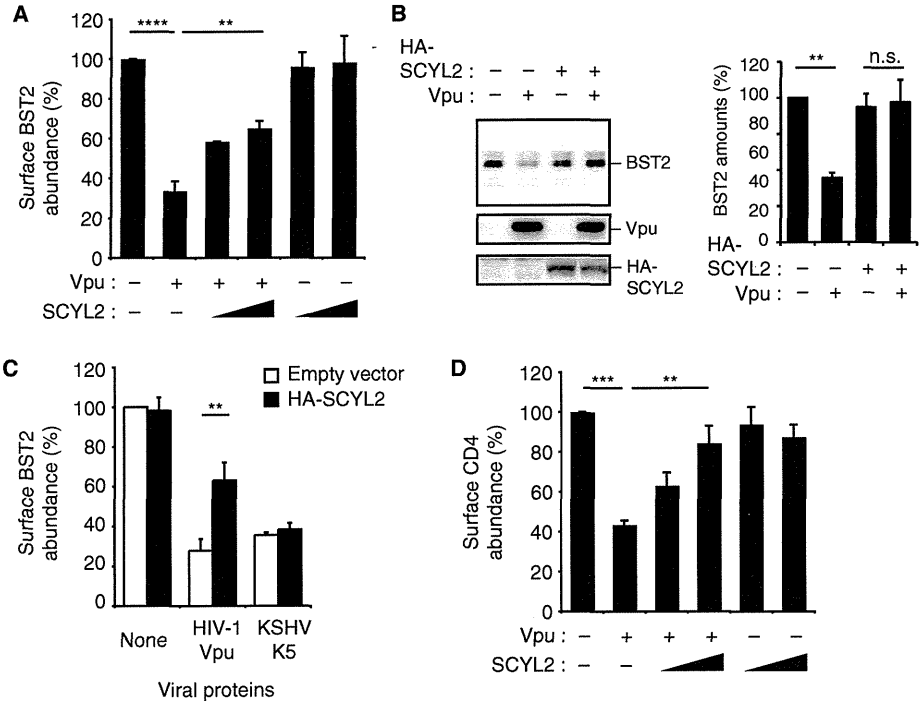


Fig. 3. SCYL2 inhibits the Vpu-induced reduction in BST2 abundance at the cell surface. (A) HeLa cells were transfected with combinations of plasmids encoding Vpu (0 and 100 ng) and hemagglutinin (HA)–SCYL2 (0, 500, and 1000 ng). The cell-surface abundance of BST2 was measured by flow cytometry. ****$P < 0.0001$; **$P = 0.0077$; $n = 3$ experiments. (B) HeLa cells were cotransfected with plasmids encoding Vpu and HA-SCYL2 at a molar ratio of 1:10. Cell lysates were processed for Western blotting analysis with anti-BST2, anti-Vpu, and anti-HA antibodies (left). Representative blots of three experiments are shown. The bar chart indicates the amounts of BST2 as determined by densitometric analysis of Western blots. n.s., not significant; **$P = 0.0020$; $n = 3$ experiments. (C) Selective inhibition of Vpu by SCYL2. HeLa cells were cotransfected with plasmid encoding HA-SCYL2 together with plasmids encoding the indicated viral proteins. After 18 hours, cell-surface BST2 abundance in the presence or absence of HA-SCYL2 was measured by flow cytometry. **$P = 0.0045$; $n = 3$ experiments. (D) SCYL2 inhibits the Vpu-induced down-regulation of CD4. H9 cells were transfected with combinations of plasmids encoding Vpu (0 and 100 ng) and HA-SCYL2 (0, 500, and 1000 ng). The cell-surface abundance of CD4 was quantified by flow cytometry. ***$P = 0.0002$; **$P = 0.0083$; $n = 3$ experiments.

of Vpu phosphorylation on $Ser^{52}$ and $Ser^{56}$ (Fig. 4C). Conversely, the targeted depletion of endogenous SCYL2 increased the amounts of phosphorylated Vpu (pVpu) (Fig. 4D). To confirm whether the effect of SCYL2 was mediated by dephosphorylation of Vpu, we treated cells with the CKII inhibitor DRB to suppress the phosphorylation of Vpu on $Ser^{52}$ and $Ser^{56}$. Treatment with DRB decreased the extent of Vpu phosphorylation, and it inhibited the reduction of cell-surface BST2 abundance by Vpu (fig. S2). Together, these results suggested that SCYL2 inhibited Vpu phosphorylation on $Ser^{52}$ and $Ser^{56}$, crucial residues for the function of Vpu in the reduction of BST2 abundance, as well as that of CD4.

## Both the kinase-like domain and the clathrin-binding domain of SCYL2 are required for its anti-Vpu activity

To verify the association between Vpu and SCYL2 in cells, we next examined the intracellular localization of both proteins by immunofluorescence confocal microscopy. Our results indicated the colocalization of SCYL2 and Vpu in the perinuclear region and cytoplasm (Fig. 5A). We confirmed a direct interaction between SCYL2 and Vpu in vitro with glutathione *S*-transferase (GST) pull-down analysis, which showed that SCYL2 copurified with GST-tagged Vpu (Fig. 5B). We next attempted to determine the binding domain of SCYL2 responsible for its interaction with Vpu in experiments with several truncation mutants of SCYL2 (Fig. 5C). SCYL2 contains an N-terminal kinase-like domain (KLD) and a C-terminal clathrin-binding domain (CBD) (*50–52*). Immunoprecipitation analysis demonstrated that Vpu coprecipitated with either full-length SCYL2 or its two C-terminal truncation mutants, termed SCYL2(N) and SCYL2(ΔCBD), but not with the N-terminal truncation mutant SCYL2(ΔKLD) (Fig. 5C). These results indicated that Vpu interacted with the KLD of SCYL2. We next examined which portions of SCYL2 were important for the dephosphorylation of Vpu and for viral restriction. Our functional analysis demonstrated that SCYL2(ΔKLD) failed to inhibit the activity of Vpu, which was consistent with its inability to bind to Vpu (Fig. 5, D and E). SCYL2(N) and SCYL2(ΔCBD) were also unable to suppress the function of Vpu (Fig. 5, D and E), potentially as a result of their inability to bind to clathrin. These data suggested that both the KLD and CBD of SCYL2 were required for its function.

SCYL2 affects the transport of intracellular proteins through its role in clathrin-mediated membrane trafficking (*51*). The SCYL2 CBD is functionally indispensable because of its association with the clathrin heavy chain (CHC) and the consequent localization of SCYL2 to clathrin-coated vesicles (*51*). To investigate whether clathrin-dependent membrane traffic was necessary for the effects of SCYL2 on Vpu, we performed experiments with cells transfected with CHC-specific siRNA. SCYL2-mediated dephosphorylation of Vpu was inhibited in CHC-depleted cells compared to that in control cells (Fig. 5F). Immunofluorescence analysis further revealed that the depletion of CHC resulted in the diffuse cytoplasmic localization of SCYL2, consistent with a previous report (*51*), and the lack of colocalization of SCYL2 with Vpu (Fig. 5G). These results suggested that clathrin-mediated membrane trafficking is required for the function of SCYL2 as an inhibitor of Vpu.

To address whether the SCYL2-Vpu interaction might be conserved during viral evolution, we investigated the association of SCYL2 with $SIV_{GSN}$ Vpu, an ancient predecessor of HIV-1 Vpu. Amino acid sequence alignment revealed that $SIV_{GSN}$ Vpu lacked the phospho-acceptor sites that correspond to $Ser^{52}$ and $Ser^{56}$ in HIV-1 Vpu (fig. S3A). We found no observable interaction between $SIV_{GSN}$ Vpu and SCYL2 (fig. S3B). Furthermore, cotransfection of cells with plasmids encoding SCYL2 and $SIV_{GSN}$ Vpu did not revert the anti-BST2 activity of $SIV_{GSN}$ Vpu, whereas SCYL2 antagonized the activity of HIV-1 Vpu (fig. S3, C and D). These

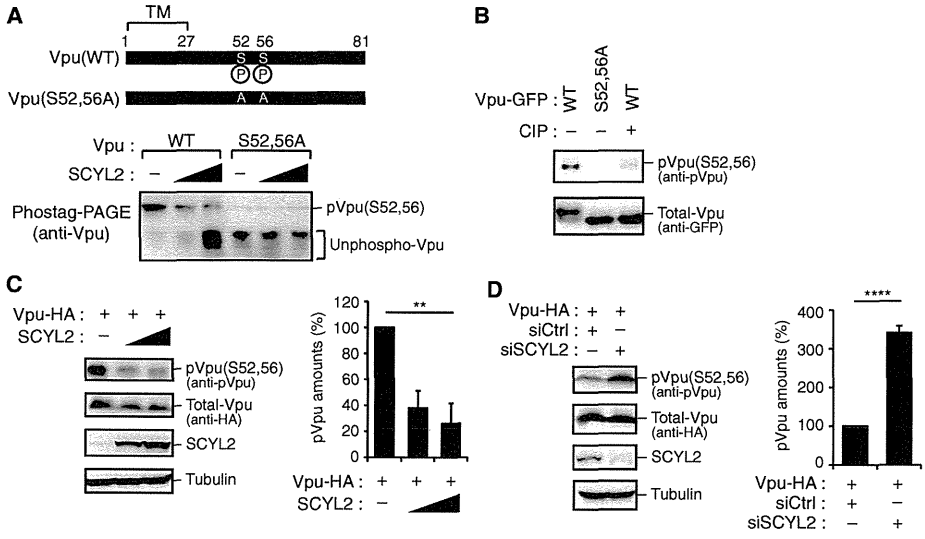


Fig. 4. SCYL2 inhibits the phosphorylation of Vpu on $Ser^{52}$ and $Ser^{56}$. (A) Schematic representation of Vpu phosphorylated at $Ser^{52}$ and $Ser^{56}$ and of alanine substitution mutants at these sites. HEK 293T cells were cotransfected with plasmids encoding either WT Vpu or the Vpu(S52,56A) mutant (100 ng) together with the SCYL2 expression plasmid (at 0, 500, or 1000 ng). Forty-eight hours after transfection, cell lysates were subjected to Phos-tag PAGE analysis. Blots were incubated with anti-Vpu antibody. (B) Specific recognition of pVpu by an anti-pVpu($Ser^{52,56}$) antibody. HEK 293T cells were transfected with expression plasmids encoding GFP-tagged WT Vpu or the Vpu(S52,56A) mutant. Twenty-four hours after transfection, cell lysates were incubated with buffer alone or with calf intestinal alkaline phosphatase for 30 min before Western blotting analysis was performed with the indicated antibodies. (C) SCYL2 facilitates the dephosphorylation of Vpu on $Ser^{52}$ and $Ser^{56}$. HEK 293T cells were transfected with plasmids encoding Vpu-HA and SCYL2 at a molar ratio of 1:5 or 1:10. Twenty-four hours after transfection, cell lysates were processed for Western blotting analysis with antibodies against the indicated proteins. The bar chart indicates the amounts of pVpu as determined by densitometric analysis of Western blots. $^{**}P = 0.0012$. (D) HEK 293T cells were treated with either control (siCtrl) or SCYL2-specific siRNA (siSCYL2) for 24 hours before being transfected with 100 ng of Vpu expression plasmids. Cell lysates were subjected to Western blotting analysis with antibodies against the indicated proteins. The bar chart indicates the amounts of pVpu as determined by densitometric analysis of Western blots. $^{****}P < 0.0001$. All data are from single experiments and are representative of three experiments.

data suggested that the interaction between SCYL2 and Vpu might have developed during the evolution of primate lentiviruses.

## SCYL2 promotes PP2A-mediated dephosphorylation of Vpu

Our earlier results suggested that SCYL2 interacted with Vpu and inhibited its function by promoting the dephosphorylation of Vpu at residues $Ser^{52}$ and $Ser^{56}$. To investigate the molecular mechanism underlying this process, we next addressed whether SCYL2 had phosphatase activity toward $Ser^{52}$ and $Ser^{56}$ on Vpu. To this end, we incubated SCYL2 immunoprecipitates with either phosphorylated or nonphosphorylated Vpu peptide containing $Ser^{52}$ and $Ser^{56}$ (AEDp$S^{52}$GNEp$S^{56}$EGE) and then measured the amounts of free phosphate released. We found that SCYL2 immunoprecipitates had phosphatase activity toward $Ser^{52}$ and $Ser^{56}$ on Vpu, which was blocked by a phosphatase inhibitor, okadaic acid (OA) (Fig. 6A). Furthermore, treatment of cells with OA blocked SCYL2-mediated dephosphorylation of Vpu and inhibition of viral release (Fig. 6, B and C). Because OA specifically inhibits the activity of PP2A in vivo, we next asked whether PP2A physically associated with SCYL2. The core structure of PP2A consists of a scaffold A subunit (PP2A/A) and a catalytic C subunit ($PP2A_C$) (*53*). Immunoprecipitation analysis revealed that SCYL2 specifically interacted with PP2A/A, but not with $PP2A_C$ (Fig. 6D), suggesting the possibility that SCYL2 recruits the scaffold subunit of PP2A to Vpu. As expected, in the presence of SCYL2, the interaction between Vpu and PP2A/A was enhanced (Fig. 6E). Moreover, Vpu interacted with endogenous SCYL2 and PP2A in HEK 293T cells (Fig. 6F). Depletion of PP2A/A by specific siRNA abrogated the SCYL2-mediated dephosphorylation of Vpu (Fig. 6G). Furthermore, immunofluorescence analysis revealed that SCYL2 induced the colocalization of PP2A/A with both Vpu and SCYL2 in the perinuclear region (Fig. 6H). These observations suggested that SCYL2 promoted Vpu dephosphorylation by recruiting PP2A to pVpu.

## SCYL2 affects Vpu function through a phosphorylation-dependent mechanism

Several studies have suggested that the mechanism by which BST2 antagonizes Vpu function is partly independent of β-TrCP and BST2 degradation (and therefore partly independent of the phosphorylation of $Ser^{52}$ and $Ser^{56}$) (*54*, *55*). We thus explored the possibility that SCYL2 might affect Vpu function through a phosphorylation-independent mechanism. To this end, we first investigated whether SCYL2 associated with the nonphosphorylated form of Vpu. Immunoprecipitation analysis demonstrated that both wild-type Vpu and the Vpu(S52,56A) mutant interacted with endogenous SCYL2 (fig. S4A). We next addressed whether SCYL2 interfered with the direct interaction between Vpu and BST2 and thereby inhibited viral release. Bimolecular fluorescence complementation analysis (*56*, *57*) revealed that SCYL2 did not interfere with the association of BST2 with either wild-type Vpu or the Vpu(S52,56A) mutant in live cells (fig. S4C). In contrast, viral release assays demonstrated that overexpression of SCYL2 inhibited the release of wild-type HIV-1 but not of its derivative encoding the Vpu(S52,56A) mutant (fig. S4, D and E). Together, these data suggested that SCYL2 interfered with the anti-BST2 activity of Vpu through a phosphorylation-dependent mechanism.

## SCYL2 affects the type I IFN–mediated antiviral response

BST2 acts as a key effector of the type I IFN–inducible antiviral response (*58*). We thus investigated whether SCYL2 might also affect this response. We treated epithelial (HeLa) and $CD4^+$ T lymphocyte (H9) cell lines with type I IFN (that is, IFN-α and IFN-β) for 6 hours and then analyzed the expression of SCYL2 by reverse transcription polymerase chain reaction (RT-PCR) or Western blotting analysis. Type I IFN increased the abundance of SCYL2 mRNA and protein in both cell lines (Fig. 7A). Moreover, analysis of reporter gene expression revealed that the 5′ untranslated region of the gene encoding